Received: 27 March 2018 | Revised: 27 August 2018 | Accepted: 3 September 2018

DOI: 10.1002/gj.3347

RESEARCH ARTICLE

WILEY

Turbidite, debrite, and hybrid event beds in submarine lobe deposits of the Palaeocene to middle Eocene Kapit and Pelagus members, Belaga Formation, Sarawak, Malaysia

Galih Yudha Kuswandaru[1] | Meor H. Amir Hassan[1] | Liviu C. Matenco[2] | Nur I. Taib[1] | Khairul A. Mustapha[1]

[1] Department of Geology, University of Malaya, Kuala Lumpur, Malaysia

[2] Faculty of Geosciences, Utrecht University, Utrecht, The Netherlands

Correspondence
Meor H. Amir Hassan, Department of Geology, University of Malaya, Kuala Lumpur 50603, Malaysia.
Email: meorhakif@um.edu.my

Funding information
University of Malaya Research Grant, Grant/Award Numbers: RP031A-15AFR and RU-011/2013

Handling Editor: M Pattaci

Turbiditic flysch units of the Rajang Group form a large crescentic belt of deformed strata in central Borneo. Unfortunately, our understanding of its bed type characteristics and depositional setting is very poor. Here, we present a detailed bed type analysis of the Palaeocene to middle Eocene Kapit and Pelagus members of the Belaga Formation, based on detailed investigations of recent road-cut exposures around Sibu, Sarawak, Malaysia. Five bed types are identified from the studied sections, representing deposition from turbidity currents, debris flows, and flows that show turbulent and laminar characteristics. The Belaga Formation deposits are divided into four bed type associations based on bed type assemblages, bed geometry, degree of bed amalgamation, vertical grain size, and bed thickness trends, for example, lobe axis, lobe off-axis, lobe fringe, and slump. Hybrid event beds (HEBs) are not restricted only to the lobe fringe but are also a common element of the lobe axis sub-environment in the Belaga Formation system. Their common occurrence in a proximal location in the lobes is probably due to enhanced seafloor erosion and rapid deceleration due to loss of confinement at the channel lobe transition further up-dip. Evidence such as bidirectional ripple cross-lamination in thin-bedded turbidites and variable palaeocurrent orientations suggest a complex depositional topography, which also suppressed flow turbulence and promoted deposition of hybrid event beds in proximal locations through deflection and deceleration of incoming flows by confining counter slopes. Similar bed type assemblages within the slump and lobe deposits indicate a local origin for the slumps. Localized failures can form on low gradient slopes developed in tectonically active basins with complex topography.

KEYWORDS

Belaga Formation, debrites, depositional lobes, distribution trends, hybrid event beds, turbidites

1 | INTRODUCTION

The Rajang Fold-Thrust Belt is the largest tectonic element in Borneo (Moss, 1998). It forms a NE–SW trending, approximately 200 km wide and almost 600 km long, crescent-shaped belt along central Borneo (Figure 1). The Rajang Fold-Thrust Belt comprises deformed Cretaceous to Paleogene flysch deposits and the strata form prominent ridges, which are clearly observed from satellite imagery. The flysch belt has been interpreted as representing an accretionary prism associated with subduction of the Proto-South China Sea during the Cretaceous, followed by continental collision and remnant ocean basin deposition during the Paleogene (Hutchison, 1996; Moss, 1998). Unfortunately, our understanding of the detailed sedimentary features, including stratal architecture, bed type composition, and

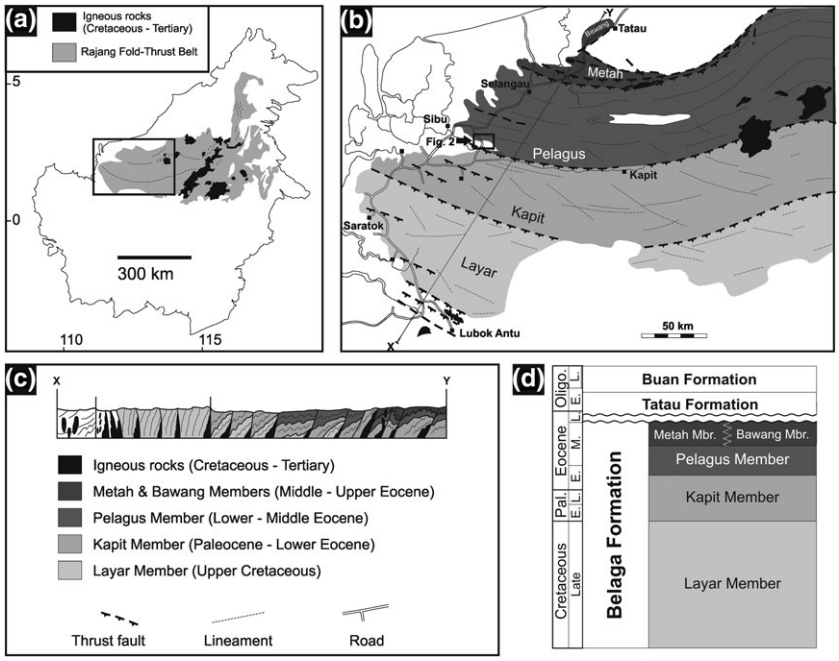

FIGURE 1 (a) Map of Borneo showing the distribution of the Rajang Fold-Thrust Belt. Based on Moss (1998) and Tate (2001). (b) Geological map of central Sarawak, showing the distribution and structural trend of the members of the Belaga Formation, Rajang Group, modified from Tongkul (1997). The regional dip is southward, but the strata young northward. Members of the Belaga Formation are bounded by imbricate thrust faults. (c) NNE–SSW oriented geological cross-section of Central Sarawa, location shown in Figure 1 b. (d) Simplified Cretaceous-Oligocene stratigraphic framework for central Sarawak, Malaysia

depositional setting of the flysch deposits, is very poor. This is mainly because of the patchy outcrop distribution, which is a result of the combined factors of wide area, slow pace of development (low population density and few roads), rugged terrain, and dense tropical vegetation. Recent civil engineering projects around the Sibu area of central Sarawak have resulted in numerous exposures of Paleogene strata of the Belaga Formation, which is the predominant stratigraphic unit of the Rajang Fold-Thrust Belt in Sarawak. These new outcrops provide an opportunity to study the detailed bed type composition and stratal arrangement of the deep-water deposits of the unit. This paper has three main objectives: (a) to present a detailed bed type analysis of deep-water deposits of the Palaeocene to middle Eocene Kapit and Pelagus members, Belaga Formation; (b) to interpret the depositional setting of the Kapit and Pelagus members, Belaga Formation, using bed type characteristics; and (c) to study the distribution of hybrid event beds (HEBs) in the depositional system of the Kapit and Pelagus members, Belaga Formation.

2 | GEOLOGICAL SETTING

The Sibu Zone of central Sarawak is part of the Rajang Fold-Thrust Belt (Madon, 1999), which is an approximately 200-km-wide and 150-km-long belt composed mainly of NE–SW trending deformed deep-water deposits (Figure 1a,b, Haile, 1974). Stratigraphically, the strata of the Sibu Zone are referred to as the Rajang Group, which generally comprises highly deformed, locally slightly metamorphosed (sub- to lower greenschist bed types), deep-water clastic deposits of Late Cretaceous–Late Eocene age (Kirk, 1957). Strata of the Rajang Group are locally separated by thrust and strike-slip faults into larger thrust sheets that reach 15 km in width (Honza, John, & Banda, 2000; Tongkul, 1997). The strata commonly display steeply dipping geometries with a general northward vergence over large areas, while deformation shows a general foreland propagation sequence of thrusting by incorporating younger deposits in thrust sheets N-wards (Figure 1b). Thus, the stratigraphy becomes younger N-wards, despite the southward-directed regional dip.

The fold and thrust belt has been interpreted to be an accretionary prism of a south- to southeast-dipping subduction zone beneath NW Borneo (Hamilton, 1979; Honza et al., 2000; Rangin et al., 1990; Tongkul, 1997), while the deposition of the younger units in the Rajang Group (which are the focus of this study) has been previously interpreted to represent the effect of collision and deformation in a marginal basin (Hutchison, 1996; Moss, 1998). The high degree of deformation and abundant evidence of syn-sedimentary deformation suggest a complicated history, possibly with several regional orogenic events (Breitfeld, 2015; Hall & Sevastjanova, 2012; Wolfenden, 1960). The Late Eocene deformation and exhumation of the Rajang Group into a northward facing and younging accretionary prism with steeply dipping strata located in the middle of the entire wedge was interpreted to be part of the larger Cretaceous to Late Eocene (85–45 Ma) southward subduction of the proto-South China Sea beneath the Kuching Zone (Hutchison, 1996; Zainol, Madon, & Abdul Jalil, 2007. However, Galin, Breitfeld, Hall, and Sevastjanova (2017) proposed a model based on the offshore Sabah fold and thrust belt, where abundant syn-depositional deformation in the Rajang Group was produced by gravitational collapse, and subsurface strata were strongly deformed and metamorphosed by strike-slip tectonics possibly related to movement along the Lupar Line.

The Rajang Group is stratigraphically divided into two units, based on foraminifera and nannofossil biostratigraphy, which are from oldest to youngest and from south to north, the Cretaceous Lupar Formation and the Late Cretaceous–Late Eocene Belaga Formation, respectively (Liechti, Roe, & Haile, 1960). The Lupar Fault Zone forms the southern boundary of the Sibu Zone to the north with the forearc deposits widely observed in the Kuching Zone southwards (Tan, 1979). The Late Cretaceous–Late Eocene Belaga Formation (Liechti et al., 1960) is widely exposed in the area between Tatau and Sibu, in central and

southwest Sarawak (Figure 1b, Kirk, 1957; Wolfenden, 1960) and is generally composed of 4.5–7.5-km-thick deep-water turbidite successions (or "flysch") made up of steeply dipping and strongly folded beds of sandstone/metasandstone interbedded with mudstone/slate/phyllite (e.g., Haile, 1969; Hutchison, 1988, 1996, 2005; Zainol et al., 2007). The Belaga Formation is subdivided into five members that show generally younger ages northwards, namely, the Late Cretaceous Layar Member, the Palaeocene-Early Eocene Kapit Member, the Early–Middle Eocene Pelagus Member, Middle–Late Eocene Metah Member, and the Late Eocene Bawang Member (Kirk, 1957; Liechti et al., 1960; Wolfenden, 1960; Figure 1b). The contact between the members is commonly a thrust fault marking isolated imbricate blocks (Honza et al., 2000; Tongkul, 1997). The Palaeocene–Early Eocene Kapit Member (Kirk, 1957; Wolfenden, 1960) consists mainly of steeply dipping and rhythmically interbedded argillites (including slates and phyllites) and sandstones, with rare conglomerates. The Kapit Member comprises thick sandstone and conglomerate in its lower part, and interbedded mudstone, slate, rare phyllite, and sandstone in its upper part interpreted as distal turbidites (Hutchison, 2005). The Pelagus Member (Early–Middle Eocene, Kirk, 1957) forms an approximately 40-km-wide belt extending to the ESE of Sibu (Figure 1b) and is predominantly argillaceous, with associated sandstones and conglomerates.

The Rajang Group, including the Belaga Formation, represents the deposits of a large submarine fan located in a remnant ocean basin or seaway (Dickinson, 1974; Moss, 1998), commonly referred to as the proto-South China Sea, Rajang Sea/Basin, or Danau Sea (e.g., Hutchison, 1996). Regional palaeogeographical reconstructions, palaeocurrent, and provenance analysis of the Rajang Group suggest a Triassic source of sediments from the Tin Belt of Peninsular Malaysia in the west and also possibly from Borneo itself, and a Cretaceous source from the Schwaner Mountains of Kalimantan in the south (Breitfeld, 2015; Galin et al., 2017; Honza et al., 2000; Hutchison, 1992, 1996, 2005).

A previous bed analysis focused on selected outcrops of the Metah, Pelagus, and Bawang members of the Belaga Formation (seven outcrops of approximately 130-m-thick logged section, Zainol et al., 2007). This work identified three main bed types: debrites, basin-floor or "distal" turbidites, and hemipelagic–pelagic deposits. Zainol et al. (2007) applied a generalized submarine fan model based on Mutti, Ricci Lucchi, and Roveri (2002) and interpreted a middle to outer fan setting for the deposits, based on the absence of channel fill deposits and the tabular stratal geometry. This initial bed types analysis is used as the basis for our detailed bed types study of the Kapit and Pelagus members of the Belaga Formation exposed around Sibu, Sarawak.

3 | METHODOLOGY

Ten well-preserved profiles (total thickness of 536 m) were logged (standard method with a Jacob's staff and compass clinometer) in the Kapit and Pelagus members of the Belaga Formation along a 12-km stretch of the Durin Road in Sibu Jaya, Sibu, Sarawak (Figure 2). The outcrops are road-cuts and are relatively small (less than 90 m long and only up to 30 m high). The strata were divided into bed types (e.g., Mueller, Patacci, & Giulio, 2017) based on bed types assemblage and vertical arrangement, vertical textural changes, and bed geometry. The degree of bioturbation was also recorded (Bioturbation Index [BI] from 0 (*no bioturbation*) to 6 (*complete bioturbation*; Taylor & Goldring, 1993). Interpretation of the observed bed types is based on the deposit-based classification scheme of density flows as proposed by Lowe (1982), Mulder and Alexander (2001), Baas, Best, Peakall, and Wang (2009), Haughton, Davis, McCaffrey, and Barker (2009), Talling, Masson, Sumner, and Malgesini (2012), Southern, Kane, Warchoł, Porten, and McCaffrey (2017), and by many other authors (see references therein). The bed types were grouped into bed type associations based on the characteristic bed type assemblage and arrangement, bed geometry, degree of bed amalgamation, and vertical trends in grain size and bed thickness. These bed type associations were subsequently used to define a new depositional model for the Kapit and Pelagus members of the Belaga Formation in the studied area.

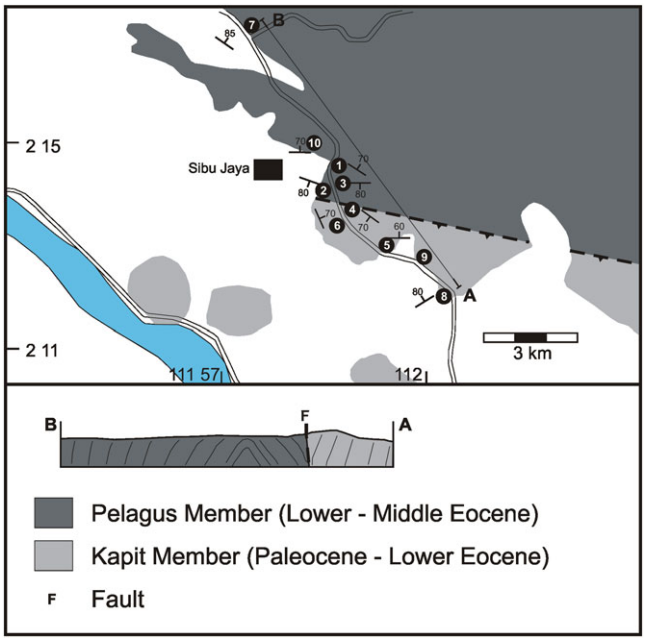

FIGURE 2 Generalized geological map of the study area, near Sibu Jaya, Sibu, Sarawak (location marked on Figure 1b). Outcrop locations are marked on the map. The studied outcrops are part of the Palaeocene to Eocene Kapit and Pelagus members, Belaga Formation [Colour figure can be viewed at wileyonlinelibrary.com]

4 | BED TYPES

Five bed types were identified from the 10 studied sections of the Kapit and Pelagus members, Belaga Formation, exposed around Sibu Jaya, Sarawak.

Bed type BT1 (*mudstone*; Figure 3a,b) is characterized by dark coloured mudstone up to 1 m thick, displaying planar bedding and sharp or gradual contacts with the overlying and underlying strata. In many cases, it overlies graded sandstone (BT2; Figure 3b). The mudstone ranges from structureless to laminated with silt and very fine sand laminae, or streaks and lenses of very fine sand. Some mudstone intervals contain lenses of sandstone (up to 1 cm thick) with

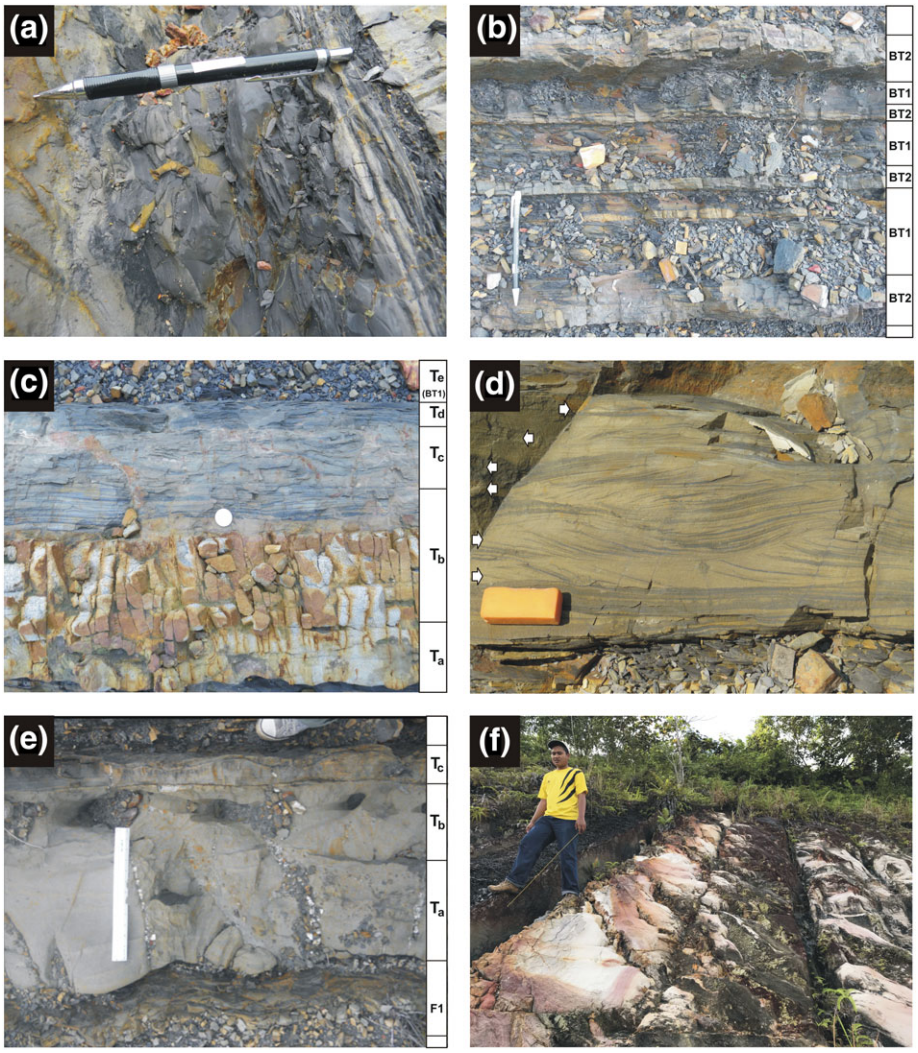

FIGURE 3 Bed types of the Palaeocene–Middle Eocene Kapit and Pelagus members, Belaga Formation of the Rajang Group, from outcrops near Sibu Jaya, Sibu, Sarawak. (a) Mudstone (BT1); (b) interbedded mudstone (BT1) and thin-bedded, graded sandstone (BT2). BT2 is interpreted as T_{CD} and T_C turbidites, with BT1 representing the T_E division. (c) Medium-bedded, graded sandstone (BT2) interpreted as low density T_{ABCD} turbidite, with overlying BT1 mudstone representing the T_E division. (d) Medium-bedded, graded sandstone (BT2) with bidirectional ripple cross-lamination in the T_C division. (e) Thick-bedded, graded sandstone, interpreted as T_{ABC} turbidite, with overlying BT1 mudstone representing the T_E division. (f) Stacked succession of structureless sandstone facies (BT3), interpreted as high density turbidites. Pencil for scale is 13 cm long. Eraser in Figure 4d is 4 cm long. Ruler in Figure 4e is 30 cm long [Colour figure can be viewed at wileyonlinelibrary.com]

asymmetrical ripple profiles and cross-lamination. The degree of bioturbation is generally low and trace fossils are mainly in the form of *Chondrites*.

Bed type BT1 is interpreted as mainly hemipelagic deposits produced by slow and continuous background sedimentation. It is generally difficult to differentiate between structureless mudstone deposited from slow and continuous background sedimentation (hemipelagic mudstone) and mudstone deposited layer by layer by a gradually waning turbulent flow (turbidite mudstone). It is also possible that some BT1 intervals are turbidite mudstones, in particular those intervals with high carbonaceous content (consistent with rapid deposition of terrigenous sediments from turbidity currents, e.g., Talling, Amy, Wynn, Blackbourn, & Gibson, 2007; Talling et al., 2012). The presence of fine-grained laminae in other examples is characteristic of the $T_{E\text{-}1}$ division of Talling et al. (2012). The formation of laminated mudstone has been explained by incremental floc settling, with the break-up of flocs, leading to size segregation of silt and clay particles (Stow & Bowen, 1978; Stow & Bowen, 1980). Ripple sandstone lenses in the mudstone are interpreted as distal expressions of the T_C division of Bouma (1962), representing dilute turbidites. The ripple lenses encased in BT1 probably represent depletion of sand supply in the distal margins of a low density turbidite, followed by reworking by the overlying muddy flow (Talling et al., 2007). The trace fossil *Chondrites* is a common constituent of various subtidal marine ichnofacies, including the *Cruziana*, *Zoophycos*, *Nereites*, and *Glossifungites* ichnofacies (MacEachern, Bann, Pemberton, & Gingras, 2007).

Bed type BT2 (*graded sandstone*; Figure 3b–e) is characterized by tabular (at the outcrop scale), sharp-based sandstone beds displaying normal grading. The bed type can be divided into three variants, based mainly on differences in bed thickness, grain size, and vertical arrangement of sedimentary structures. Thin-bedded (1–15 cm thick) variants of BT2 typically grade upwards from fine-grained sand to silt, before

being gradually overlain by mudstone of BT1 (Figure 3b). Individual beds display a vertical sedimentary structure arrangement from basal parallel laminated sandstone into ripple cross-laminated sandstone and parallel laminated siltstone. Sandstone beds thinner than 3 cm are characterized by ripple cross-lamination, which are sharply overlain by mudstone of BT1.

Medium-bedded variants of BT2 are 15–30 cm thick and grade upward from medium- to fine-grained sand. The beds are poorly sorted and grey in colour. Medium-bedded BT2 variants typically display an upward trend from parallel laminated sandstone, into ripple cross-laminated sandstone and parallel laminated siltstone. In some rare examples, there is a basal structureless sandstone overlain by parallel-laminated sandstone (Figure 3c). Also, in some examples, the parallel laminated sandstone interval is characterized by gently undulating parallel lamination. Successive layers of ripple cross-laminated sandstone can form amalgamated stacks up to 40 cm thick and display opposing foreset dip orientations (Figure 3d).

Thick-bedded variants of BT2 are 50–150 cm thick and also grade upward from medium- to fine-grained sand (Figure 3e). The base is sharp, commonly scoured and displays groove casts. Small (less than 3 cm long) angular mud rip-up clasts are locally present near the base of some of the beds but are not abundant. The typical sedimentary structure arrangement is from structureless sandstone at the base, into parallel laminated sandstone, ripple cross-laminated sandstone, and parallel laminated siltstone. Some examples, from base to top, display a trend from structureless sandstone that is directly overlain by ripple cross-laminated and finer-grained sandstone. Individual ripple layers also display normal grading from fine to very fine sand. Ball-and-pillow structures, as well as fluid escape structures, are commonly observed in the thick-bedded BT2 variant. In some cases, the BT2 beds also display an upward increase in mud clast concentration, with mud clasts becoming more abundant at the top of the bed. In some examples, several beds of BT2 are amalgamated and form stacks up to 7 m thick.

Bioturbation is observed in the thin-bedded variant of BT2, where it is sparse and includes *Paleodictyon*, *Cosmorhaphe*, and *Chondrites*.

Bed type BT2 is interpreted as turbidites deposited by non-cohesive dilute turbidity currents, based on the sharp-based, normal graded beds and vertical arrangement of sedimentary structures consistent with turbidity current bed type models (Bouma, 1962; Lowe, 1982). The normal grading of beds records the gradual decrease in flow velocity and flow turbulence, grain size segregation, and incremental deposition characteristic of turbidity currents (Bouma, 1962; Lowe, 1982; Talling et al., 2012). The characteristic vertical organization of sedimentary structures in the BT2 beds roughly conform to the classical Bouma (1962) and Lowe (1982) divisions for turbidites, which record deposition from a waning flow. Complete T_{ABCDE} and T_{BCDE} sequences record the temporal transition from high density to low density turbidity current deposition (e.g., Bouma, 1962; Lowe, 1982). Scours and groove casts indicate erosive, high energy, and high density conditions. The presence of ball-and-pillow structures and fluid escape structures in T_A are consistent with rapid sediment fallout, which resulted in near-bed liquefaction due to excess pore pressures as the rate of deposition exceeded the rate of pore fluid escape (Lowe, 1982). Fine-grained planar lamination of T_B is interpreted as either the deposit of high density turbidity current traction carpets, or upper stage plane bedforms associated with a dilute, low density turbidity current (e.g., Best & Bridge, 1992; Lowe, 1982; Mutti, 1992; Sumner, Amy, & Talling, 2008). Currently, it is not possible to differentiate between planar lamination generated by high or low density turbidity currents based on bed type characteristics observed in outcrop. Sumner et al. (2008) suggested that the boundary between underlying high density turbidity current deposition and overlying low density turbidity current deposition probably occurs within the T_B interval. The ripple cross-laminated sandstone interval (T_C) is interpreted as deposition from a dilute and low density turbidity current, where the low rate of sediment fallout resulted in the development of ripple bedforms. The origin of the laminated siltstone (T_D) interval is still uncertain, although the finer grain size relative to the underlying Tc sandstone is consistent with deposition from the progressively waning dilute flow of a low density turbidity current. Lowe (1982) suggested that laminae developed because of insufficient time for bedload reworking to form ripples.

Incomplete T_{BCDE}, T_{CDE}, and T_E sequences of the medium- and thin-bedded BT2 variants are interpreted as representing the deposits of only dilute and low density turbidity currents. Bidirectional ripple cross-laminations in the T_C division of medium-bedded BT2 may indicate reworking by bottom currents (e.g., Ito, 1996; Shanmugam, 2013) or flow reflection. Intervals of undulating parallel-lamination in the T_C division of medium-bedded turbidites are similar to the ones observed in the Upper Cretaceous Basque Basin, where they have been interpreted to either be the product of turbidity current reflection or Kelvin–Helmholtz instability formed at the upper flow interface of turbidity currents (Mulder et al., 2009). The thin-bedded turbidites (BT2) were probably deposited from the end tail of long-lived, high energy and high density turbidity currents, which extended from a submarine fan system and thinned out onto the distal lobe fringe. Thin-bedded BT2 turbidites with a basal T_C interval sharply overlain by BT1 mudstone marks a grain size break. Grain size breaks between T_C and overlying T_E mudstone are common in low density turbidites (Bouma, 1962; Gladstone & Sparks, 2002; Migeon et al., 2001; Talling, Amy, & Wynn, 2007) and have been interpreted as the product of sediment bypass associated with a transition from non-cohesive to cohesive (floc) settling (e.g., Piper, 1978; Talling et al., 2012).

Variations in grain size range, Bouma division arrangement, and bed thickness are mainly a function of differences in flow velocity, turbulence, and sediment availability. It is possible that the variations record deviations in distance and energy, with thicker, more complete Bouma sequences being located in a more proximal location, while thinner sequences preserving only the uppermost divisions recording deposition from a more dilute flow in a relatively more distal setting. The trace fossil assemblage comprising *Paleodictyon*, *Cosmorhaphe*, and *Chondrites* is indicative of the *Nereites* ichnofacies, which is characteristic of deep-marine settings (e.g., MacEachern et al., 2007).

Bed type BT3 (*structureless sandstone*; Figure 3f) is characterized by 40 cm to 5-m-thick beds of well sorted medium- to fine-grained sandstone. The beds are typically tabular, but some examples display a scoured, concave upward basal profile with dm-scale relief. BT3 does not display any obvious grading. The sandstone is commonly

sharply overlain by BT1 mudstone. BT3 also commonly forms amalgamated stacks up to 10 m thick.

Bed type BT3 is interpreted as high density turbidites and is similar in nature to the basal T_A structureless sandstone of BT2 and the S_3 turbidite division of Lowe (1982). The structureless sandstone interval is interpreted as representing deposition from a high density turbidity current, with rapid fallout resulting in insufficient time to produce bedforms (Kuenen, 1966; Lowe, 1982; Middleton & Hampton, 1973; Talling et al., 2012).

Bed type BT4 (*muddy*, *clast-rich sandstone*; Figure 4) is characterized by 40 cm to 3-m-thick, tabular beds of grey to dark grey, argillaceous, poorly sorted, medium- to fine-grained sandstones. The base of the sandstone is typically scoured. BT4 commonly contains abundant outsized, chaotically arranged mudstone and sandstone clasts floating in a muddy sandstone matrix, with the clasts generally making up between 10% and 30% of the bed. The sandstone clasts have deformed shapes and contain parallel and ripple cross-lamination. The size of the clasts varies, with sub-rounded clasts being comparably smaller in size than angular clasts. The angular clasts range between 1 and 30 cm in size, while the sub-rounded clasts range between 1 and 10 cm.

Bed type BT4 is interpreted as representing cohesive debris flow deposits (debrites), based on the structureless and ungraded texture of the sandstone beds, the presence of significant amount of argillaceous matrix in the beds, and the abundance of chaotically oriented mudstone and sandstone clasts. The structureless ungraded texture of the beds is consistent with abrupt *en masse* deposition. The presence of argillaceous matrix supporting chaotically oriented larger clasts in relatively thin tabular beds, indicate inefficient sorting and *en masse* deposition from a moderate strength cohesive debris flow (Hodgson, 2009; Talling et al., 2012). Downslope flow of sediment–water mixture can erode, entrain, and rework sediment from underlying beds, resulting in broken up clasts being transported together further downslope. Flow reduction and eventual depletion downslope stopped the movement of the fluid when the frictional force was greater than the flow of the fluids (Arnott, 2010).

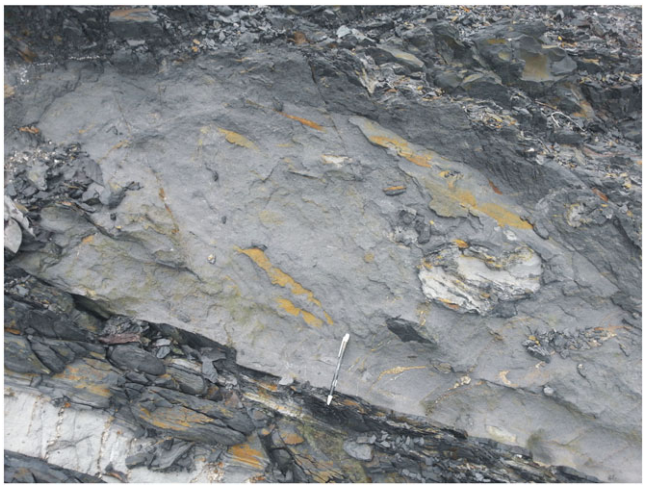

FIGURE 4 Muddy, clast-rich sandstone (BT4), with clasts composed of sandstone and mudstone. BT4 is interpreted as debrite. Pencil for scale is 13 cm long [Colour figure can be viewed at wileyonlinelibrary.com]

Bed type BT5 (*bipartite to tripartite beds*; Figure 5) are 30–60 cm thick and are mainly composed of medium- to very fine-grained and poor to moderately sorted sandstone. The beds also display sharp upper and lower contacts towards overlying and underlying beds. The base can either be planar or erosional, with less than 1-cm relief.

BT5 beds in the Belaga Formation show a bipartite to tripartite vertical bed organization, with different upper and lower bed characteristics. BT5 can be divided into two sub-types, based on differences in the bed divisions (referred to hereon as bed intervals *sensu* Jackson, Zakaria, Johnson, Tongkul, & Crevello, 2009). BT5a has a bipartite bed organization, with intervals separated by a sharp boundary (Figure 5b–d). The lower interval of the bed is typically represented by medium- to fine-grained structureless sandstone. The lower interval structureless sandstone also displays dewatering sheets and occasionally exhibits weak normal grading. Locally, basal parts of the lower interval feature parallel lamination. Mud clasts are rare but when present are small and randomly scattered in the sandstone. The overlying upper interval comprises of poorly sorted muddy sandstone, which is commonly clast rich, with the clasts being matrix supported. The upper interval displays a more recessively weathered appearance in the field, relative to the blocky underlying lower interval. Clasts in the upper interval are mainly mud clasts, although sandstone clasts and clasts preserving heterolithic bedding are also present. The clasts are typically smooth-edged, elongate (up to tens of centimetres long), and oriented parallel to bedding. The mud clasts are also sporadically deformed. The very fine-grained muddy sandstone matrix is grey to dark grey in colour and poorly sorted. The matrix commonly displays a swirly fabric, with deformed patches of cleaner sand and areas with finely dispersed carbonaceous matter. Convolute bedding is present in clast-rich zones of the muddy sandstone.

The boundary separating the upper and lower intervals is sharp. The boundary is commonly irregular and displays loading and injection of the lower interval sand into the upper interval. On rare occasions, large, and elongate mud clasts are concentrated at the boundary between the lower and upper intervals.

BT5b is similar to BT5a in the presence of the lower and upper intervals. However, BT5b displays a tripartite structure, with the muddy sandstone upper interval being overlain by a thin interval of fine-grained and ripple cross-laminated to parallel laminated sandstone (Figure 5e).

Bed type BT5 is interpreted as displaying evidence of co-genetic flow behaviour. The BT5 beds record changes between laminar and turbulent flow states in a sediment gravity flow, based on the bipartite to tripartite bed structure, with an argillaceous, clast-rich sandstone interval in close vertical association with structureless sandstone and normal graded sandstones displaying incomplete Bouma sequences (Davis et al., 2009; Fisher, 1983; Haughton et al., 2009; Haughton, Barker, & McCaffrey, 2003; Hodgson, 2009; Ito, 2008; Magalhaes & Tinterri, 2010; Patacci, Haughton, & McCaffrey, 2014; Talling, Amy, Wynn, Peakall, & Robinson, 2004). BT5a and BT5b record deposition from an initially turbulent flow, which is overlain by the deposit of a later, co-genetic, cohesive, laminar flow. Structureless sandstone of the lower interval in BT5a and BT5b is interpreted as a high density turbidite (T_A), based on the sand-rich matrix, structureless bed and weak normal grading. Occasional occurrence of parallel lamination in the lower

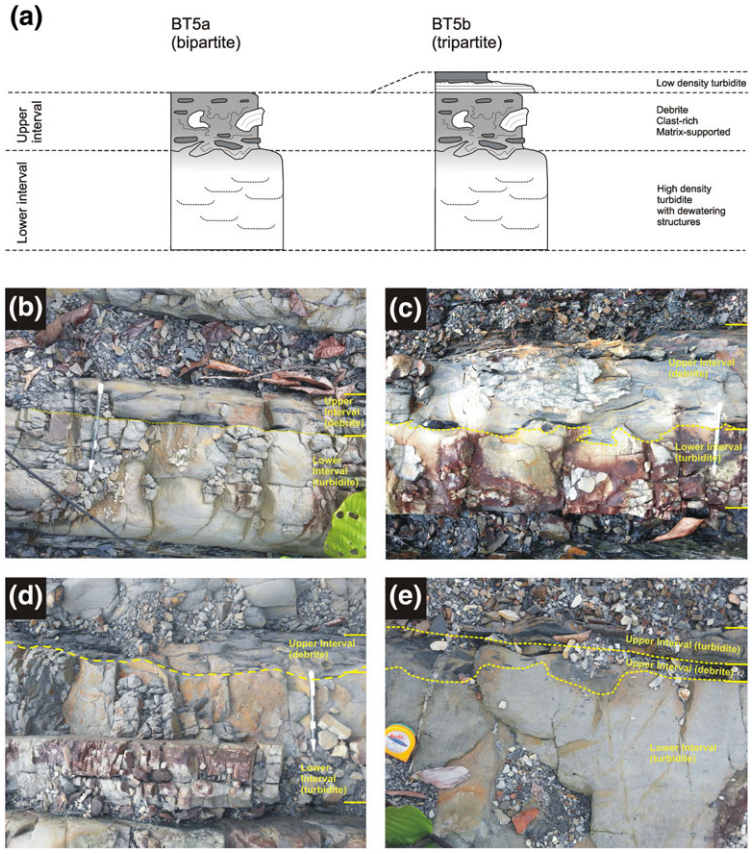

FIGURE 5 Bipartite to tripartite beds (Facies BT5) of the Palaeocene–Middle Eocene Kapit and Pelagus members, Belaga Formation, Rajang Group, exposed near Sibu Jaya, Sibu, Sarawak. (a) Simplified diagram of BT5, showing the division of individual beds into a lower interval characterized by structureless sandstone with dewatering structures, and an overlying upper interval characterized by a muddy, clast-rich sandstone. In some examples of BT5 (variant BT5b), the muddy, clast-rich sandstone is overlain by a thin, normal graded sandstone displaying ripples and/or plane-parallel lamination. These hybrid, bipartite to tripartite beds record flow transformation, from non-cohesive turbidity current (lower interval), into a cohesive debris flow (upper interval muddy, clast-rich sandstone), with the overlying thin graded sandstone representing a waning turbulent flow. (b–d) BT5a variant. Notice the sharp and irregular boundary between lower interval turbidite and upper interval debrite, with associated load and fluid injection structures. (e) BT5b variant, with a thin T_C turbidite overlying the upper interval debrite. Pencil for scale is 13 cm long [Colour figure can be viewed at wileyonlinelibrary.com]

interval is also consistent with traction and grain segregation below a turbidity current (Bouma division T_B). Rare mud clasts indicate incorporation of basin floor mud or from a muddy substrate further up-dip, through erosion by the turbulent flow. The overlying upper interval is interpreted as a debrite, based on the structureless ungraded and matrix-rich character of the sandstone beds, and the abundance of chaotically organized mudstone and sandstone clasts. The systematic repeated association in BT5a and BT5b of turbidite sandstone overlain by debrite is consistent with a genetic relationship between the upper and lower intervals, with the different intervals representing separate but temporally closely related flow phases within a single gravity flow event (Fonnesu, Felletti, Haughton, Patacci, & McCaffrey, 2018; Fonnesu, Haughton, Felletti, & McCaffrey, 2015; Fonnesu, Patacci, Haughton, Felletti, & McCaffrey, 2016; Haughton et al., 2003, 2009; Hodgson, 2009). The gravity flow event was originally fully turbulent (lower interval) but evolved into a cohesive, laminar debris flow (upper interval "linked debrite," *sensu* Haughton et al., 2003), with the debris flow phase travelling on the previously deposited turbidite sand bed. The common occurrence of dewatering structures in the lower interval sandstone, sand injections penetrating into the upper interval and deformed clasts in the upper interval provide evidence for active dewatering during overriding debrite emplacement, thus supporting emplacement of the debrite immediately after deposition of the lower interval turbidite. The presence of concentrations of mud clasts below the upper interval muddy sandstone is consistent with flow transformation through erosional bulking, where the initially turbulent flow is charged with mud clasts, which disintegrate, increasing the clay concentration of the flow and suppressing turbulence (Fonnesu et al., 2015, 2016, 2018; Haughton et al., 2003; Kane et al., 2017). These bipartite to tripartite beds are referred to in the literature as hybrid event beds (HEBs), with the upper interval muddy sandstone referred to as a "linked" debrite (Haughton et al., 2003, 2009). Jackson et al. (2009) refer to such beds as "co-genetic turbidite-debrite beds." The ripple cross-laminated sandstone layer capping the upper interval debrite in the tripartite beds is interpreted as representing low density T_C turbidites, deposited from a trailing and waning turbulent cloud, which marks a return to non-cohesive behaviour of the flow (Haughton et al., 2009). There are four main interpretations for the formation of such hybrid event beds (Haughton et al., 2003; Talling et al., 2004). The first mechanism involves simultaneous or retrogressive failure of sandy and heterolithic slopes, resulting in the deposition and stacking of unrelated debrites and turbidites (Masson, Van Niel, & Waever, 1997; Nelson, Twichell, Schwab, Lee, & Kenyon, 1992; Patacci et al., 2014; Wood & Smith, 1958). However, this mechanism is considered the least likely, because it would produce randomly arranged beds, rather than the commonly observed turbidite with linked debrite hybrid event beds (Haughton et al., 2009). The second mechanism requires an initial debris flow which is developed up-dip due to slope failure. The debris flow is then partially transformed downslope into a turbidity current, which moves faster than the debris flow (Haughton et al., 2003). The tail-end debris flow then catches up and overlies the forerunner turbidity current. The third mechanism uses incorporation of clay into the initial non-cohesive turbidity current to explain its transformation into a cohesive debris flow (Haughton et al., 2003). Incorporation of clay is through erosion of the seafloor by the initial turbidity current (Baas & Best, 2002; Haughton et al., 2003; Sumner, Talling, & Amy, 2009; Talling, 2013; Talling et al., 2004). The fourth mechanism involves turbulence segregation and suppression. The vertical velocity gradient of a turbidity

current results in vertical segregation of suspended material based on differences in grain density, size, and shape (Altinakar, Graf, & Hopfinger, 1996; Garcia, 1994; Garcia & Parker, 1993; Kneller & Buckee, 2000; Stacey & Bowen, 1988). Coarser sediment around the velocity maximum is transported at a higher velocity, while slower settling particles above the velocity maximum are segregated towards the rear of the current (longitudinal segregation). Progressive enrichment of the tail of the turbidity current with fine-grained material and flow deceleration eventually results in suppression of turbulence and transformation of the rear end flow into a laminar, cohesive debris flow (Baas & Best, 2002; Fonnesu et al., 2018; Haughton et al., 2009; Kane et al., 2017; Kane & Pontén, 2012). The significant transport distance required for flow transformation and clay incorporation through the second and third mechanism are regarded to explain the predominance of hybrid event beds in distal fan settings.

5 | BED TYPE ASSOCIATIONS (BTA)

The limited lateral extent of individual outcrops, strong tectonic deformation, and poor biostratigraphic control hinders correlation between outcrops in the study area. Bed type associations are identified in the study area based on bed type assemblages, bed geometry, degree of bed amalgamation, vertical grain size, and bed thickness trends. We apply an outcrop-based classification scheme of depositional lobe sub-environment, which is in part based on schemes proposed by Hodgson et al. (2006), Prélat, Hodgson, and Flint (2009), and Prélat and Hodgson (2013) for sand-rich depositional lobes of the Tanqua depocentre, Karoo Basin. In this scheme, individual depositional lobes can be subdivided into three main sub-environments, according to their relative distance to the feeder channel supplying sediment to the lobe, listed from proximal/axial to frontal/lateral, respectively: (a) lobe axis; (b) lobe off-axis; and (c) lobe fringe. Four bed type associations are recognized in the study area (BTA 1 Lobe axis, BTA 2 Lobe off-axis, BTA 3 Lobe fringe, and BTA 4 Slump; Figures 6–11).

Bed type association BTA 1 (Figure 6a) forms up to 25-m-thick successions, which generally consist of high density turbidites (BT3), with minor interbedded mudstone and thin- to medium-bedded turbidites (BT1 and BT2), and rare debrites (BT4). BT3 commonly form amalgamated stacks up to 10 m thick. Bed geometry is generally tabular in outcrop. However, many BT3 beds also display an erosional base with a concave-upward profile, with associated sole marks. Intervals of interbedded BT1 and BT2 separate the amalgamated BT3 beds and are 1 to 4.5 m thick. Vertical successions of BTA 1 tend to show a blocky or thinning and fining-upward pattern. Hybrid event beds (BT5) are common in BTA 1 examples observed in logged section 2 (Figure 8). The hybrid event beds are abundant at the base of the BTA 1 successions and are overlain by amalgamated beds of BT3. Palaeocurrent readings obtained from sole marks indicate a general northward flow direction (Figures 8 and 10).

Bed type association *BTA 1 is interpreted as lobe axis* deposits, based on the mainly tabular geometry, with intercalated, subordinate channel-like geometries observed in outcrop, the predominance of high density turbidite deposition and the high degree of bed amalgamation. We acknowledge that identification of depositional elements in the Belaga Formation is difficult, due to the limited exposure of outcrops. However, the predominance of tabular geometries in the turbidite sandstones is consistent with an unconfined submarine depositional lobe setting. The predominance of sand-dominated high density turbidites and high degree of sandstone bed amalgamation is used as evidence for an axial position in the depositional lobe (Grundvåg, Johannessen, Helland-Hansen, & Plink-Björklund, 2014; Lowe, 1982; Prélat et al., 2009; Spychala, Hodgson, Prelat, et al., 2017). BT3 intervals displaying scoured bases with concave-upward profiles are interpreted as shallow channel bodies. The thin interbedded BT1 and BT2 intervals are interpreted as possible inter-lobe or inter-lobe element deposits, which either represent intervening periods of low sediment supply, or the distal fringe deposits of a separate but laterally adjacent depositional lobe (e.g., Prélat & Hodgson, 2013). A similar association of amalgamated sheet turbidite sandstone and minor intercalated channel turbidite sandstones is observed in the turbidite system of the Tanqua sub-basin, Karoo Basin, South Africa (Johnson, Flint, Hinds, & Wickens, 2001). The bed type association in the Karoo is described as a transitional depositional style occupying a proximal and axial position on depositional lobes. This interpretation is consistent with our observations in the Belaga Formation. The shallow channelized turbidite beds are interpreted as representing the down-dip termination of distributary channels (Johnson et al., 2001; Terlaky, Rocheleau, & Arnott, 2016). There is increasing evidence that gravity flow transformations, from turbidity flow to cohesive and laminar flow, are the dominant bed type in the distal ends of submarine fan systems and the fringes of individual lobes (e.g., Barker, Haughton, McCaffrey, Archer, & Hakes, 2008; Fonnesu et al., 2018; Grundvåg et al., 2014; Haughton et al., 2003, 2009; Hodgson, 2009; Ito, 2008; Kane & Pontén, 2012; Lowe & Guy, 2000; Pierce et al., 2017; Spychala, Hodgson, & Lee, 2017; Sylvester & Lowe, 2004; Talling et al., 2004). However, they are not exclusively restricted to the distal parts and can also be present in proximal areas of lobes, where they are interpreted as the product of enhanced erosion and flow deceleration due to processes occurring in the channel-lobe transition and due to basin confinement (e.g., Fonnesu et al., 2018; Haughton et al., 2009; Ito, 2008; Jackson et al., 2009; Mueller et al., 2017; Patacci et al., 2014; Sylvester & Lowe, 2004; Terlaky et al., 2016; Vinnels, Butler, McCaffrey, & Lickorish, 2010).

Bed Type Association BTA 2 is known only from two examples in logged sections 2 and 6 (Figures 6c, 8, and 9). BTA 2 is up to 20 m thick and is mainly composed of interbedded high density turbidites (BT3), hybrid event beds (BT5), and mudstone (BT1). Sandstone beds are occasionally amalgamated to form stacks up to 3 m thick, but overall, BTA 2 is poorly amalgamated. Bed geometry is tabular.

The bed type association *BTA 2 is interpreted as lobe off-axis* deposits based on the mainly tabular bed geometry, the high sand content but with relatively low degree of bed amalgamation relative to BTA 1, and the predominance of high density turbidites. The lower degree of bed amalgamation suggests a more basinward or lateral position relative to BTA 1. At the individual lobe scale, the lower degree of amalgamation of turbidites is characteristic of an off-axis lobe setting relative to BTA 1, that is, laterally or distally away from the main distributary channel supplying sediment (i.e., off-axis; Prélat et al., 2009). Again, as in BTA 1, the presence of HEBs in BTA2 provides further record of this bed type in proximal locations of lobes.

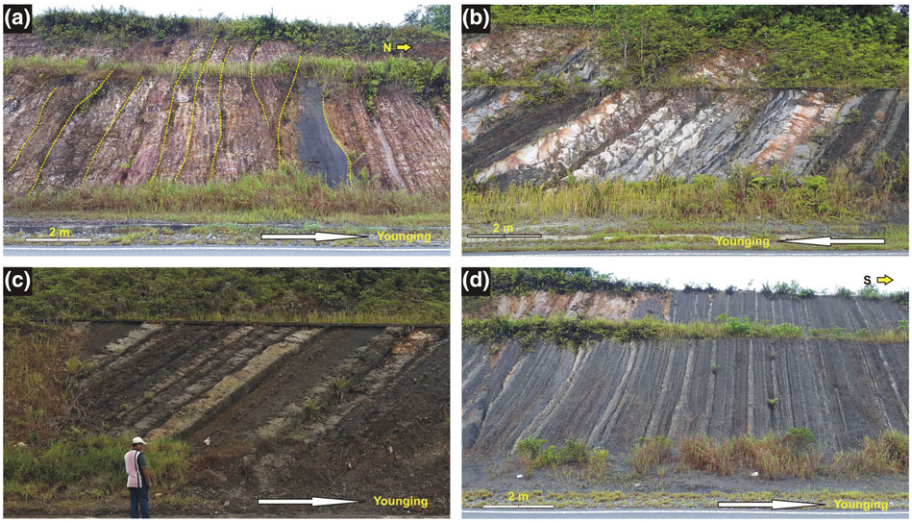

FIGURE 6 Bed type associations of the Palaeocene–Middle Eocene Kapit and Pelagus members, Belaga Formation, exposed near Sibu Jaya, Sibu, Sarawak. (a) Bed type association BTA 1 displaying amalgamated turbidite sandstone beds. Some of the beds display concave-upward, scoured bases. BTA 1 is interpreted as lobe axis deposits. Outcrop location 8, Kapit Member. (b) BTA 1 displaying a sand-dominated succession, comprising abundant hybrid event beds in the lower part, overlain by amalgamated turbidite sandstone beds. Outcrop location 3, Pelagus Member. (c) Bed Type Association BTA 2 composed of poorly to non-amalgamated beds of high density turbidites, hybrid beds and interbedded mudstone. BTA 2 is interpreted as lobe off-axis deposits. (d) Bed type association BTA3 composed of interbedded mudstone, thin- to medium-bedded turbidite, hybrid event beds and debrite facies. BTA 3 is interpreted as lobe fringe deposits. Outcrop location 8, Kapit Member. Refer to Figure 2 for outcrop locations [Colour figure can be viewed at wileyonlinelibrary.com]

The bed type association BTA 3 (Figure 6d) forms 5- to 65-m-thick successions which display either no systematic vertical pattern in grain size or bed thickness, or an upward fining and bed thinning trend. The bed type association is typically dominated by mudstone of BT1, which is commonly intercalated with cm- to dm-thick low density turbidites (BT2), dm-thick high density turbidites (BT3), dm-thick debrites (BT4) and bipartite to tripartite, and hybrid event beds (BT5). BTA 3 displays some variability in turbidite bed thickness, with numerous bed thinning/thickening trends throughout the succession. In the fining and bed thinning upward examples of BTA 3, the hybrid event beds (BT5) are more common in the lower part of the succession. The beds are commonly tabular with no significant basal erosion. However, erosional scours do occur locally.

The bed type association *BTA 3 is interpreted as lobe fringe* deposits, based on the tabular geometry of sandstone beds, the predominance of mudstone bed type, the relatively thin nature of the turbidite and hybrid event beds and the absence of bed amalgamation (e.g., Prélat & Hodgson, 2013; Spychala, Hodgson, Prelat, et al., 2017). The predominance of the mudstone bed type (BT1), the mainly dm-scale thickness of individual sandstone beds and the absence of bed amalgamation, indicates a more basinward or lateral position relative to BTA 2. At the individual lobe scale, hybrid event beds are common elements of the lobe fringe area (Fonnesu et al., 2018; Grundvåg et al., 2014; Haughton et al., 2003, 2009; Hodgson, 2009; Ito, 2008; Kane & Pontén, 2012; Pierce et al., 2017; Spychala, Hodgson, & Lee, 2017; Talling et al., 2004). Bed thinning upward patterns may indicate either lobe/fan retreat (i.e., retrogradation), across-strike lobe/fan shifting (i.e., avulsion), or a combination of both (Prélat & Hodgson, 2013; Spychala, Hodgson, & Lee, 2017).

The bed type association BTA 4 (Figure 7) is characterized by 1- to 15-m-thick units of interbedded turbidites and mudstone of bed types BT1, BT2, and BT3, displaying intraformational, recumbent, and asymmetric folding. The bed type assemblage of BTA 4 is similar to BTA 2. BTA 4 can be laterally extensive at the outcrop scale, with exposures up to 80 m wide. Many of the examples of BTA 4 display continuous folded layers. The folded intervals are bounded vertically by

FIGURE 7 Bed type association BTA 4 example, displaying large-scale slump folds and large, isolated blocks of sandstone with abundant soft-sediment deformation structures. Outcrop location 9, Kapit Member. Refer to Figure 2 for outcrop location [Colour figure can be viewed at wileyonlinelibrary.com]

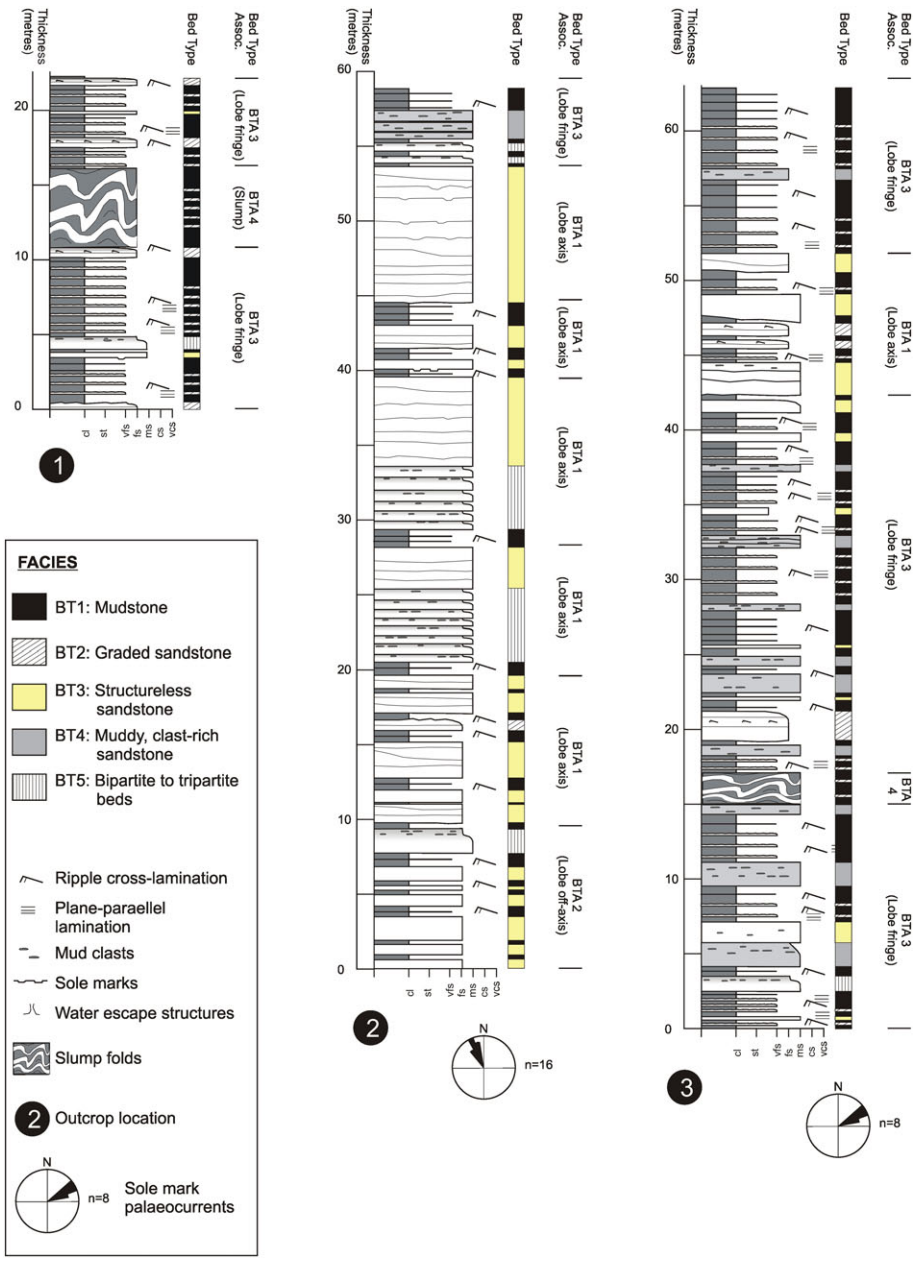

FIGURE 8 Sedimentary logs from outcrops 1–3, showing bed types and bed type associations, Eocene Pelagus Member, Belaga Formation, near Sibu Jaya, Sarawak (refer to Figure 2 for locations and Figure 8 for symbol legend). Rose diagrams display palaeocurrent readings obtained from flute casts at the base of turbidite sandstones [Colour figure can be viewed at wileyonlinelibrary.com]

undeformed strata. Other examples display discontinuous beds with pinching and swelling of the bed thickness. Some of the folded intervals are also internally faulted. Large rotated sandstone blocks (up to 5 m long) are commonly observed surrounded by folded layers of BTA 4. The sandstone blocks are typically structureless (BT3) but can contain abundant water escape structures, including dish and pillar structures, ball-and-pillow structures, and swirly lamination.

Based on internal deformation of strata and the presence of large rotated sandstone blocks, *BTA 4 is interpreted as slump* deposits formed by mass movement. Most of the thin BTA 4 intervals probably represent localized remobilization of sediment. It is likely that the larger and thicker slump exposures of BTA 4 at logged section 7 and 9 (see Figure 2 for location) are parts of large-scale mass transport complexes (e.g., Algar, Milton, Upshall, Roestenburg, & Crevello, 2011; Shipp, Weimer, & Posamentier, 2011). Characteristics of the Belaga Formation slumps which are consistent with large-scale mass transport deposition include extensive deformation of strata and the presence of blocks of various sizes (e.g., Algar et al., 2011).

6 | DEPOSITIONAL MODEL FOR THE KAPIT AND PELAGUS MEMBERS, BELAGA FORMATION

Previous workers used vertical trends in bed thickness and grain size as criteria for the identification of submarine fan depositional elements such as lobes and channels (e.g., Mutti, 1974; Pickering, 1981; Ricci-Lucchi, 1975). However, Prélat and Hodgson (2013) pointed

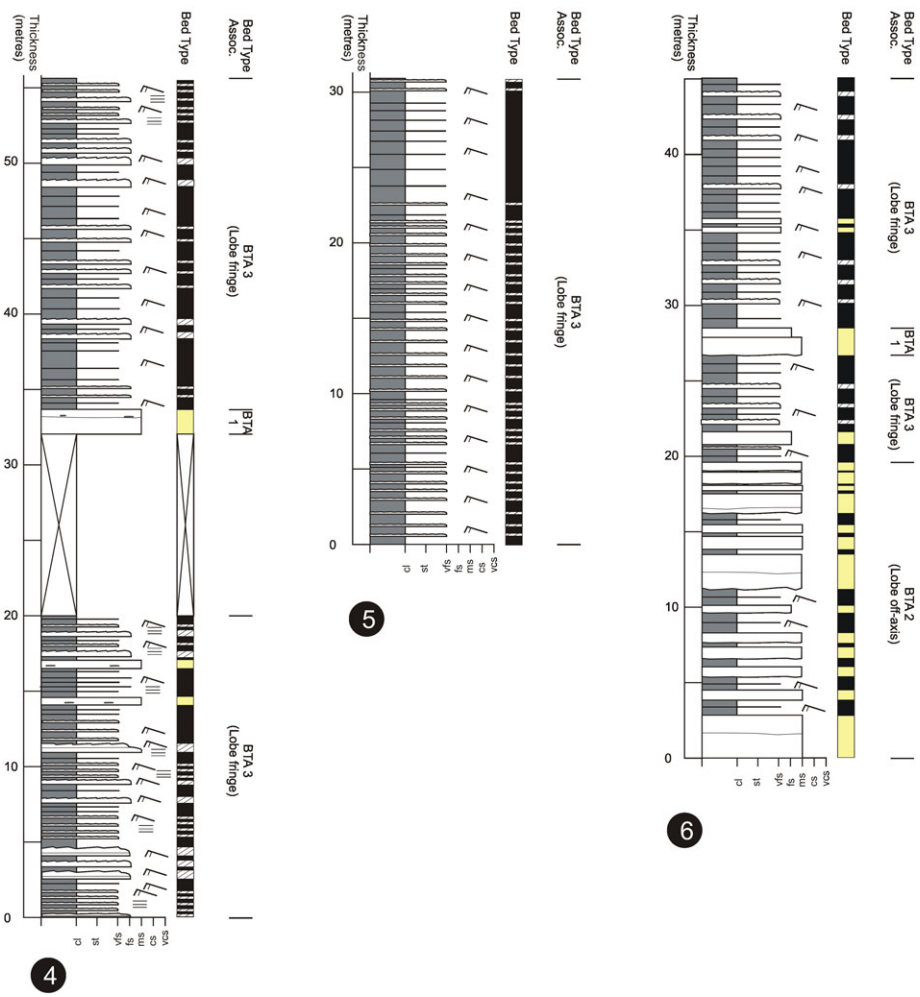

FIGURE 9 Sedimentary logs from outcrops 4–6, showing bed type and bed type associations, Palaeocene–Lower Eocene Kapit Member, Belaga Formation, near Sibu Jaya, Sarawak (refer to Figure 2 for locations and Figure 8 for symbol legend). Rose diagrams display palaeocurrent readings obtained from flute casts at the base of turbidite sandstones [Colour figure can be viewed at wileyonlinelibrary.com]

out weaknesses in the interpretation of depositional lobes using vertical bed type trends without information on lateral extent. In places with good outcrop exposures, individual lobes can be identified by mapping their bounding surfaces at the km scale (e.g., Prélat & Hodgson, 2013). There is significant variation in the vertical bed type trends of lobes, including recorded examples of coarsening and thickening upward, fining, and thinning, combination of coarsening/thickening upward followed by fining/thinning upward, to examples with no observable trend, even at different hierarchical lobe scales (e.g., Marini, Milli, & Moscatelli, 2011; Spychala, Hodgson, & Lee, 2017; Zhang et al., 2016). The limited lateral extent and two-dimensional outcrop exposure, dense vegetation, and strong deformation of strata of the Belaga Formation complicate a detailed allocation of depositional sub-environments. However, detailed bed type analysis of the deposits, as demonstrated in this work, can result in relatively good and generalized depositional models for turbidite systems in areas of limited exposure.

As concluded in the previous section, the tabular stratal geometry and the predominance of gravity flow deposits in the Belaga Formation is consistent with a deep-water submarine fan setting, in the deposition-dominated lower fan of the Pirmez, Beauboeul, Friedmann, and Mohrig (2000) model. More specifically, the bed type assemblage, tabular stratal geometry with minimal evidence of erosion is characteristic of basin floor, terminal lobe depositional elements.

The frontal and lateral bed type transition from axis to fringe is related to the gradual thinning and fining of depositional lobes. Bed type associations BTA 1 to BTA 3 in the Belaga Formation are interpreted using this scheme, where they represent lobe axis, lobe off-axis, and lobe fringe sub-environments (Figure 12). Currently, it is not possible to determine whether the bed type associations of the Belaga Formation represent either bedsets, individual lobe elements, lobes, or lobe complexes, as the identification of individual lobes and their associated architectural element hierarchies requires mapping of stratal thickness variations and the identification of lobe-bounding surfaces at the km scale (e.g., Hodgson, 2009; Prélat et al., 2009). Therefore, we use the term "lobe" for the depositional elements represented by the bed type associations in a general sense. The thickness range of bed type associations in the Belaga Formation (metres to tens of metres thick) suggests that most of them represent lobe stacks (*sensu* Marini et al., 2011; Zhang et al., 2016). For comparison, individual lobes are commonly less than 10 m thick in the Karoo Basin (Prélat, Covault, Hodgson, Fildani, & Flint, 2010). The amalgamated, scour-based sandstones of BTA 1 (lobe axis) represent the most proximal part of the Belaga Formation lobes, located down-dip of distributary channel mouths feeding sediment to the lobes.

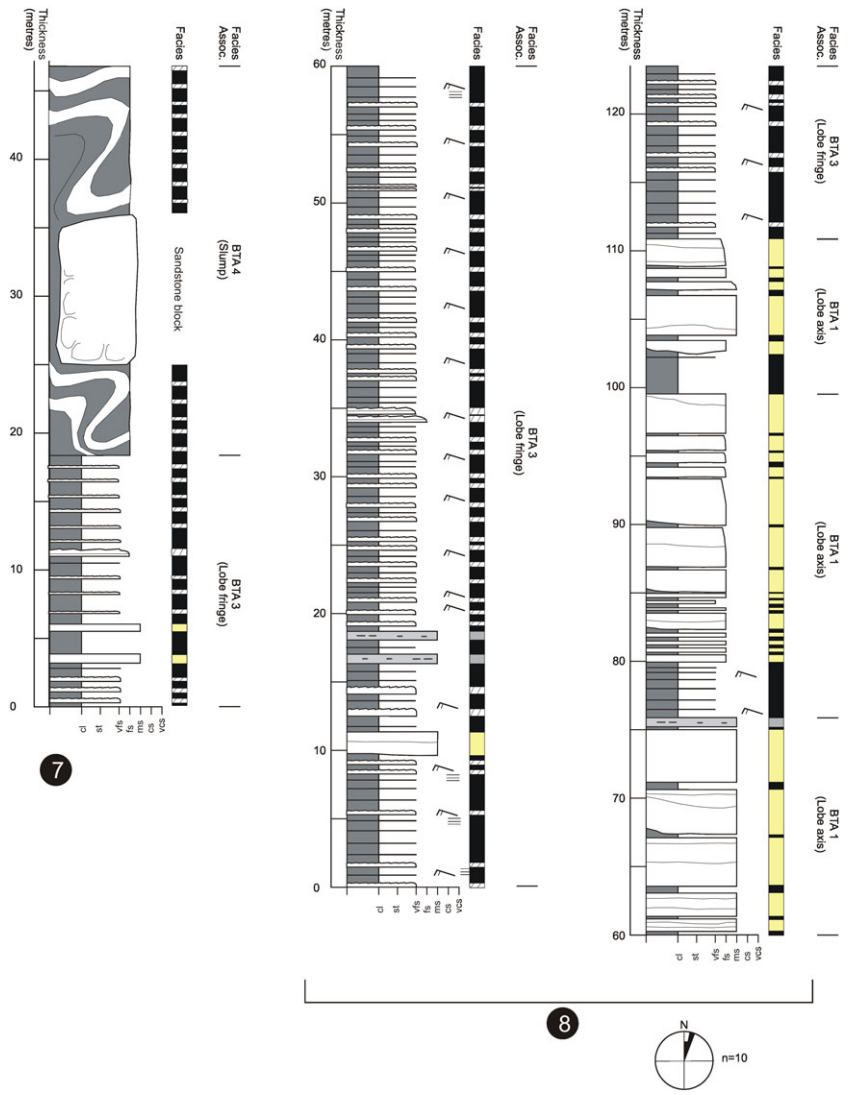

FIGURE 10 Sedimentary logs from outcrops 7 (Eocene Pelagus Member, Belaga Formation) and 8 (Palaeocene–Lower Eocene Kapit Member, Belaga Formation), near Sibu Jaya, Sarawak, showing bed types and bed type associations (refer to Figure 2 for locations and Figure 8 for symbol legend). Rose diagrams display palaeocurrent readings obtained from flute casts at the base of turbidite sandstones [Colour figure can be viewed at wileyonlinelibrary.com]

BTA 2 (lobe off-axis) is located in a more distalward or lateral position relative to BTA 1, based on the lower degree of bed amalgamation and the absence of erosional scouring (i.e., further away from the main feeder channel). Initially, the presence of extensive slump deposits in close relationship with the lobe deposits appears to be problematic. The internal bed type of the slump deposits is similar to the surrounding undisturbed strata, being mainly composed of thin-bedded turbidites, with occasional rotated blocks of thicker, high density turbidites. This supports a local origin for the slump or mass transport deposits, with localized failure of low gradient slopes, which resulted in remobilization of unconsolidated, heterolithic lobe deposits. Such low gradient slopes can be present in tectonically active basins featuring complex topography (e.g., Marini et al., 2011). Mud-dominated MTDs have been described from younger (Neogene) submarine fan systems onshore and offshore Sabah, Malaysia (e.g., Algar et al., 2011). However, these MTDs likely reflect upslope failure and are closely associated with leveed channel deposits.

The bed type analysis presented here for the the Kapit and Pelagus members of the Belaga Formation provide further evidence for the abundance of HEBs in sandier, more proximal lobe settings. Hybrid event beds are particularly common in the sand-dominated lobe axis bed type association (BTA 1) of the Belaga Formation. As discussed previously, there are four main mechanisms for hybrid flow development and deposition. The most likely explanations for hybrid event bed deposition in the Belaga Formation are erosion of muddy substrate and entrainment of the mud clasts into the flow and flow confinement. It is probable that the hybrid event beds were formed by a combination of both mechanisms, as the mechanisms for hybrid deposition can be variable even in a single basin (Fonnesu et al., 2018; Pierce et al., 2017). In the Gottero turbidite system of NW Italy, there is evidence for muddy substrate erosion and mud clast entrainment in proximal locations, based on the clast-rich character of the hybrid event beds (Fonnesu et al., 2018). In the Middle and Upper Kaza groups of the southern Canadian Cordillera, the erosion and entrainment of abundant fine-grained material was also interpreted to have occurred up-dip on a muddy seafloor, due to the rapid expansion and increased turbulence of flows downstream of avulsion nodes (Terlaky et al., 2016). Hybrid event beds of the Belaga Formation are relatively rich in mud and sandstone clasts, which appear to have a local origin. Mud clast entrainment in proximal locations leading to the development of proximal HEBs has been attributed to enhanced turbulence in the channel-lobe transition zone due to loss of confinement and flow expansion (e.g., Ito, 2008; Terlaky et al., 2016). For example, the coarse-grained sand-rich Bordighera turbidite system of

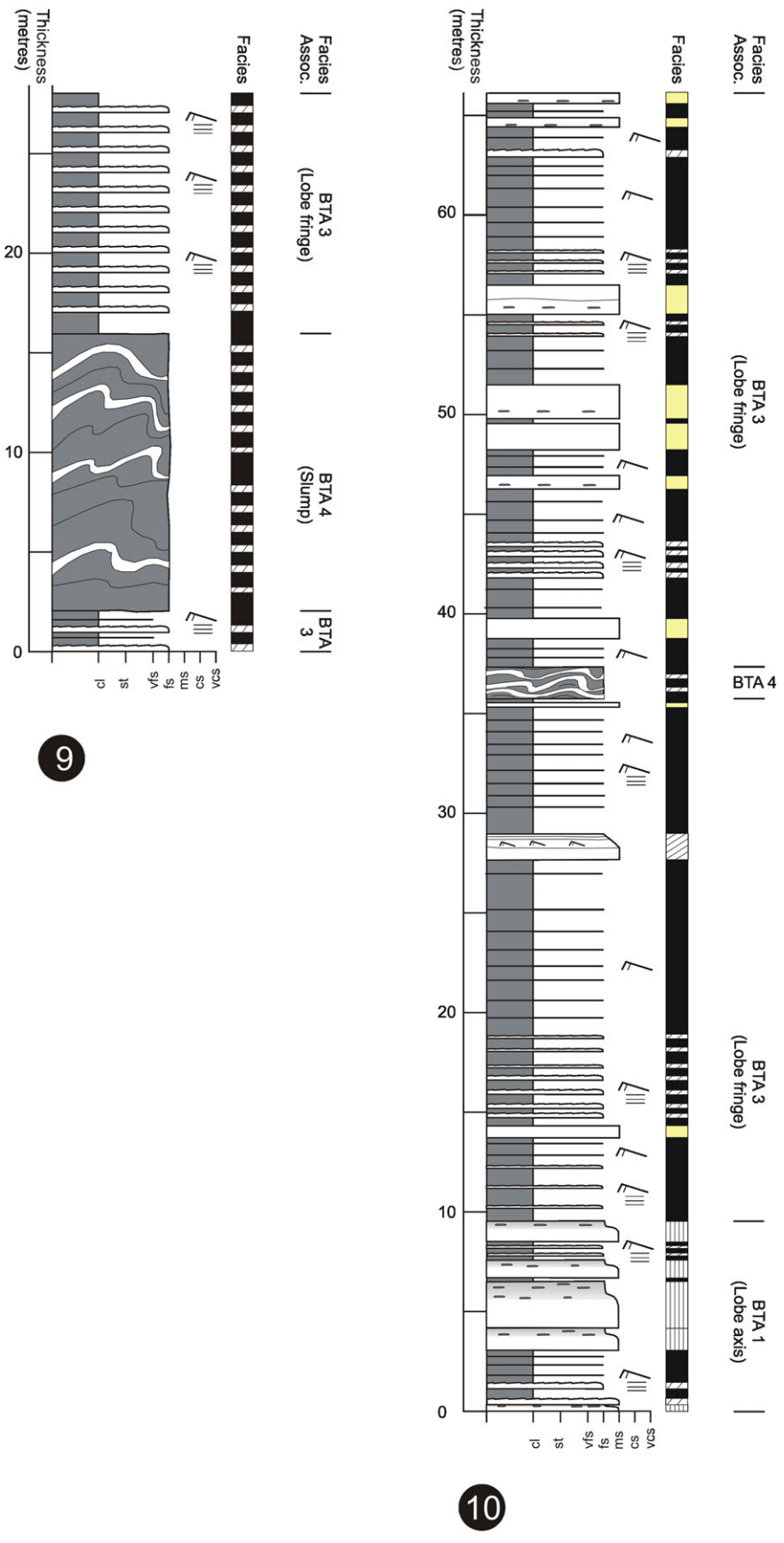

FIGURE 11 Sedimentary logs from outcrops 9 (Palaeocene–Lower Eocene Kapit Member, Belaga Formation) and 10 (Eocene Pelagus Member, Belaga Formation), near Sibu Jaya, Sarawak, showing bed types and bed type associations (Refer to Figure 2 for locations and Figure 8 for symbol legend) [Colour figure can be viewed at wileyonlinelibrary.com]

NW Italy displays an abundance of HEBs in axial/proximal lobe deposits, which have been interpreted to be a product of entrainment of basin floor mud at the channel-lobe transition zone by unconfined jet flows (Mueller et al., 2017). However, the Kapit and Pelagus member turbidite system differs from the Bordighera turbidite system in the low abundance of HEBs in the lobe off-axis sub-environment.

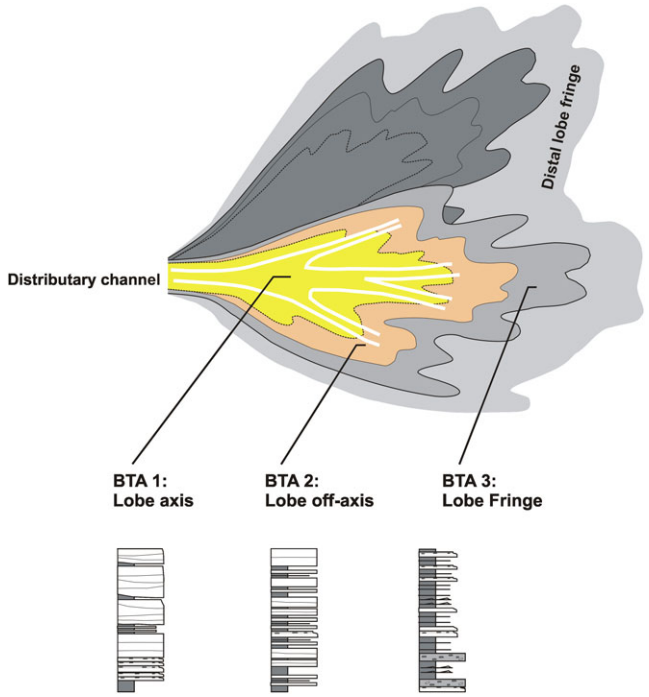

FIGURE 12 Generalized depositional model of the Belaga Formation as basin floor, terminal lobe deposits associated with a lower submarine fan setting, based on Hodgson (2009), Prélat et al. (2009), Prélat and Hodgson (2013), Kane et al. (2017), Spychala, Hodgson, & Lee, 2017, Spychala, Hodgson, Prelat, et al., 2017, and Fonnesu et al. (2018). Individual bed type associations identifed in the Belaga Formation are interpreted as representing different lobe sub-environments, with an axial-to-frontal and proximal-to-lateral transition from lobe axis, to lobe off-axis and lobe fringe. The model is generalized and does not indicate scale [Colour figure can be viewed at wileyonlinelibrary.com]

HEB development may also be influenced by depositional topography, where a change in slope gradient can result in flow deceleration (e.g., Fonnesu et al., 2018; Talling, Wynn, Masson, Frenz, et al., 2007). For example, Patacci et al. (2014) described hybrid event beds from a proximal position in the Braux Unit of the Annot sandstone of SE France. Here, the presence of a confining counter slope close to the sediment entry point into the narrow basin resulted in the deflection and deceleration of incoming flows, which triggered flow transformation and deposition of hybrid event beds. A similar interpretation was also applied to the Marnoso-arenacea Formation of northern Italy, where turbidites were deposited in tectonically confined sub-basins of a larger foredeep basin (Tinterri, Muzzi Magalhaes, Tagliaferri, & Cunha, 2016). Again, flow deceleration due to complex topography resulted in turbulence suppression and deposition of hybrid event beds. In the case of the Belaga Formation, erosion and entrainment of muddy substrate from up-dip channel-lobe transition areas and turbulence damping by down-dip basin floor topography led to the down-dip transformation of turbidity currents into increasingly cohesive flows and eventual deposition of hybrid event beds on the basin floor.

Previous palaeocurrent measurements from the older Late Cretaceous Lupar Formation (NE directed) and the Rajang Group in Kalimantan (E-ward directed) are consistent with newly collected data and have been used to interpret a generally SW–NE oriented axis for the Rajang Sea remnant ocean basin and the development of an axial submarine fan system (Moss, 1998; Tan, 1979, 1982). Thirty-four palaeocurrent measurements were taken from flute casts in the studied outcrops of the Belaga Formation. Ten readings were taken from BTA 1 (lobe axis bed type association), 16 were taken from BTA 2 (lobe off-axis bed type association), and 8 readings were taken from BTA 3 (lobe fringe bed type association) (See Rose diagram at the bottom of Logs 2, 3, and 8 in Figures 8–11). BTA 1 and BTA 2 flute casts display a general N-ward transport direction for the Belaga Formation depositional lobes. However, the lobe fringe (BTA 3) palaeocurrents indicate a NE-ward transport direction. There are two ways to interpret the change in transport direction from lobe axis to lobe fringe: (a) the sediment source was in the south, but transport direction shifted NE in the distal reaches of the lobe, parallel to the Rajang Sea axis (i.e., there was a complex sea floor topography); or (b) the variation in palaeocurrent readings may represent a radial pattern of sediment transports, consistent with a depositional lobe interpretation (i.e., a marked loss in flow confinement). Turbidity current reflection in a basin with complex topography is a good explanation for the undulating planar lamination and bidirectional ripple cross-laminations observed in the medium-bedded turbidites (e.g., Tinterri et al., 2016). The locally originated slumps also support such an interpretation. Overall, the first interpretation of complex topography of the Belaga Formation basin is most likely.

The stratigraphic distribution of the hybrid event beds in the Belaga Formation also provide further insight into the depositional setting and evolution. Hybrid event beds are observed in the lobe axis, lobe off-axis, and lobe fringe deposits. When present in lobe axis deposits, they are most abundant in the lower part of the succession, where they directly overly m-thick mudstone bed type. The hybrid event beds are overlain by amalgamated high density turbidites.

The vertical gradation from hybrid event bed-dominated to amalgamated turbidite-dominated strata observed in BTA 1 may represent either basinward migration, lateral migration, or combined basinward and lateral migration of depositional lobes (Prélat & Hodgson, 2013). The sharp change from hemipelagic mudstone into hybrid event beds rather than a gradual coarsening and thickening upward succession is interpreted as possibly representing rapid, forced progradation of a submarine lobe in an area of limited accommodation (e.g., Kane & Pontén, 2012). Hybrid event beds are rare in the lobe off-axis, but this is most likely due to the limited data sample (only two examples of BTA 2 are identified in the study area). It may also reflect higher concentration of mud entrainment in more proximal settings near the channel-lobe transition. The observed hybrid event beds are located at the top of the bed type association, which is overlain by amalgamated beds of the lobe axis (BTA 1) bed type association. This merely indicates that the depositional setting becomes more proximal up-section, with HEBs being more abundant in more proximal locations in the Belaga Formation depositional lobes. In the lobe fringe bed type association (BTA 3), hybrid event beds commonly display a sporadic distribution, interbedded between mudstone and thin bedded turbidites. However, hybrid event beds are also concentrated near the base of BTA 3 intervals directly overlying amalgamated axial lobe deposits, and also near the boundary between successive BTA 3 packages. The concentration of hybrid event beds at the boundary between bed type associations is consistent with lateral migration and progradation/retrogradation of depositional lobe stacks

due to compensational stacking, allocyclic changes in sediment sediment supply, and slope gradient and up-dip avulsion. The variability in the stratigraphic distribution of the hybrid event beds is again consistent with variability of hybrid event bed development mechanisms in the Belaga Formation depositional system.

7 | CONCLUSIONS

A detailed bed type analysis of the deep-water Palaeocene to middle Eocene Kapit and Pelagus members of the Belaga Formation exposed around Sibu, Sarawak, indicates the predominance of turbidites, debrites, hemipelagic deposits, and hybrid event beds (HEBs). Hybrid event beds comprise a lower dewatered turbidite interval overlain by a linked clast-rich debrite. They indicate downslope flow transformation from an initially non-cohesive to cohesive flow. Based on the bed type assemblage and the degree of amalgamation, the Belaga Formation is divided into bed type associations which are interpreted as representing deposition in different geographic positions within a terminal lobe setting (from axial/proximal to lateral/distal: lobe axis, lobe off-axis, and lobe fringe, respectively).

This paper documents the common occurrence of hybrid event beds in high net-sand intervals of the lobe axis deposits. Hybrid event beds are common elements of the distal parts of submarine fan systems. However, they are not exclusively distributed there. Their occurrence in proximal areas of depositional lobes in the Belaga Formation is explained by a combination of enhanced erosion and rapid deceleration around the channel-lobe transition, and turbulence suppression caused by complex basin floor topography.

ACKNOWLEDGEMENTS

The bulk of the work presented here is from Galih's MSc project, which was supported by University of Malaya Research Grant (RP031A-15AFR). We are highly indebted to Dr. Yvonne Spychala, an anonymous reviewer, and Dr. Marco Patacci for their constructive comments.

ORCID

Galih Yudha Kuswandaru http://orcid.org/0000-0002-6328-8246

REFERENCES

Algar, S., Milton, C., Upshall, H., Roestenburg, J., & Crevello, P. (2011). Mass-transport deposits of the deep-water northwestern Borneo margin-characterization from seismic-reflection, borehole and core data with implications for hydrocarbon exploration and exploitation. In R. C. Shipp, P. Weimer, & H. W. Posamentier (Eds.), *Mass-transport depostis in deep-water settings*. *SEPM Special Publication no. 96*. (pp. 351–366).

Altinakar, M., Graf, W., & Hopfinger, E. (1996). Flow structure in turbidity currents. *Journal of Hydraulic Research*, *34*(5), 713–718.

Arnott, R. W. C. (2010). Deep-Marine sediments and sedimentary systems. Facies models 4. In P. J. Noel, & W. D. Robert (Eds.), *Geological Association of Canada* (pp. 300–329).

Baas, J. H., & Best, J. L. (2002). Turbulence modulation in clay-rich sediment laden flows and someimplications for sediment deposition. *Journal of Sedimentary Research*, *72*, 336–340.

Baas, J. H., Best, J. L., Peakall, J., & Wang, M. (2009). A phase diagram for turbulent, transitional, and laminar clay suspension flows. *Journal of Sedimentary Research*, *79*, 162–183.

Barker, S. P., Haughton, P. D. W., McCaffrey, W. D., Archer, S. G., & Hakes, B. (2008). Development of rheological heterogeneity in clay-rich high-density turbidity currents: Aptian Britannia sandstone member, U.K. Continental shelf. *Journal of Sedimentary Research*, *78*, 45–68.

Best, J., & Bridge, J. (1992). The morphology and dynamics of low amplitude bedwaves upon upper stage plane beds and the preservation of planar laminae. *Sedimentology*, *39*, 737–752.

Bouma, A. H. (1962). *Sedimentology of some flysch deposits*. In *A graphic approach to facies interpretation* (p. 168). Amsterdam: Elsevier.

Breitfeld, H. T. (2015). *Provenance, stratigraphy and tectonic history of Mesozoic to Cenozoic sedimentary rocks of West and Central Sarawak, Malaysia*. PhD Thesis, Royal Holloway University of London. p. 808

Davis, C., Haughton, P., McCaffrey, W., Scott, E., Hogg, N., & Kitching, D. (2009). Character and distribution of hybrid sediment gravity flow deposits from the outer Forties Fan, Paleocene Central North Sea, UKCS. *Marine and Petroleum Geology*, *26*, 1919–1939.

Dickinson, W. R. (1974). Plate tectonics and sedimentation: Society of Economic Paleontologist and Mineralogist Special Publication 22, p.1–27.

Fisher, R. V. (1983). Flow transformations in sediment gravity flows. *Geology*, *11*, 273–274.

Fonnesu, M., Felletti, F., Haughton, P. D. W., Patacci, M., & McCaffrey, W. D. (2018). Hybrid event bed character and distribution linked to turbidite system sub-environments: The North Apennine Gottero sandstone (north-west Italy). *Sedimentology*, *65*, 151–190.

Fonnesu, M., Haughton, P., Felletti, F., & McCaffrey, W. D. (2015). Short length-scale variability of hybrid event beds and its applied significance. *Marine and Petroleum Geology*, *67*, 583–603.

Fonnesu, M., Patacci, M., Haughton, P. D. W., Felletti, F., & McCaffrey, W. D. (2016). Hybrid event beds generated by local substrate delamination on a confined-basin floor. *Journal of Sedimentary Research*, *86*, 929–943.

Galin, T., Breitfeld, T., Hall, R., & Sevastjanova, I. (2017). Provenance of the Cretaceous-Eocene Rajang Group submarine fan, Sarawak, Malaysia from light and heavy mineral assemblages and U-Pb zircon geochronology. *Gondwana Research*, *51*, 209–233.

Garcia, M. H. (1994). Depositional turbidity currents laden with poorly sorted sediment. *Journal of Hydraulic Engineering*, *120*(11), 1240–1263.

Garcia, M. H., & Parker, G. (1993). Experiments on the entrainment of sediment into suspension by a dense bottom current. *Journal of Geophysical Research*, *98*(3), 4793–4807.

Gladstone, C., & Sparks, R. S. J. (2002). The significance of grain-size breaks in turbidites and pyroclastic density current deposits. *Journal of Sedimentary Research*, *72*, 182–191.

Grundvåg, S. A., Johannessen, E. P., Helland-Hansen, W., & Plink-Björklund, P. (2014). Depositional architecture and evolution of progradationally stacked lobe complexes in the Eocene Central Basin of Spitsbergen. *Sedimentology*, *61*, 535–569.

Haile, N. S. (1969). Geosynclinal theory and the organizational pattern of the NW Borneo Geosyncline. *Journal of Geoogical Society of London*, *124*, 171–194.

Haile, N. S. (1974). Borneo. In A. M. Spencer (Ed.), *Geological Society of London. Special Publication* (Vol. 4). *Mesozoic-Cenozoic orogenic belts: Data for orogenic studies*. (pp. 333–347).

Hall, R., & Sevastjanova, I. (2012). Australian crust in Indonesia. *Australian Journal of Earth Sciences*, *59*(6), 1–18.

Hamilton, W. (1979). Tectonics of the Indonesian region 1078, U.S. Geological Survey Professional paper, (p. 345).

Haughton, P. D. W., Barker, S. P., & McCaffrey, W. D. (2003). Linked debrites in sand-rich turbidite systems—Origin and significance. *Sedimentology*, *50*, 459–482.

Haughton, P. D. W., Davis, C., McCaffrey, W., & Barker, S. (2009). Hybrid sediment gravity flow deposits—Classification, origin and significance. *Marine and Petroleum Geology*, *26*, 1900–1918.

Hodgson, D. M. (2009). Distribution and origin of hybrid beds in sand-rich submarine fans of the Tanqua depocentre, Karoo Basin, South Africa.

In L. A. Amy, W. B. McCaffrey, & P. J. Talling (Eds.), *Hybrid and transitional submarine flows* (Vol. 26). *Marine and Petroleum Geology*. (pp. 1940–1957).

Hodgson, D. M., Flint, S. S., Hodgetts, D., Drinkwater, N. J., Johannessen, E. P., & Luthi, S. M. (2006). Stratigraphic evolution of fine-grained submarine fan systems, Tanqua Depocenter, Karoo Basin, South Africa. *Journal of Sedimentary Research*, *76*, 20–40.

Honza, E., John, J., & Banda, R. M. (2000). An imbrications model for the Rajang Accretionary Complex in Sarawak, Borneo. *Journal of Asian Earth Science*, *18*, 751–759.

Hutchison, C. S. (1988). Stratigraphic-tectonic model for Eastern Borneo. 22, 135–151.

Hutchison, C. S. (1992). The Eocene unconformity in Southeast and East Sundaland. *Geological Society of Malaysia Bulletin*, *32*, 69–88.

Hutchison, C. S. (1996). The Rajang accetionary prism and Lupar Line problem of Borneo. In R. Hall, & D. Blundell (Eds.), *Tectonic evolution of South East Asia*, Geology Society of London special publication (ed., Vol. 106) (pp. 247–261).

Hutchison, C. S. (2005). *Geology of North-West Borneo*. Sarawak, Brunei, and Sabah: Elsevier Science.

Ito, M. (1996). Sandy contourites of the Lower Kazusa Group in the Boso Peninsula, Japan: Kuroshio current influenced deep-sea sedimentation in a Plio-Pleistocene forearc basin. *Journal of Sedimentary Research*, *66*, 587–598.

Ito, M. (2008). Downfan transformation from turbidity currents to debris flows at a channel-to-lobe transitional zone: The lower Pleistocene Otadai Formation, Boso Peninsula, Japan. *Journal of Sedimentary Research*, *78*, 668–682.

Jackson, C. A.-L., Zakaria, A. A., Johnson, H. D., Tongkul, F., & Crevello, P. D. (2009). Sedimentology, stratigraphic occurrence and origin of linked debrites in the West Crocker Formation (Oligo-Miocene), Sabah, NW Borneo. *Marine and Petroleum Geology*, *26*, 1957–1973.

Johnson, S. D., Flint, S. S., Hinds, D., & Wickens, H. D. V. (2001). Anatomy of basin floor to slope turbidite systems, Tanqua Karoo, South Africa: Sedimentology, sequence stratigraphy and implications for subsurface prediction. *Sedimentology*, *48*, 987–1023.

Kane, I., Pontén, A., Vangdal, B., Eggenhuisen, J., Hodgson, D. M., & Spychala, Y. T. (2017). The stratigraphic record and processes of turbidity current transformation across deep-marine lobes. *Sedimentology*, *64*, 1236–1273.

Kane, I. A., & Pontén, A. S. M. (2012). Submarine transitional flow deposits in the Paleogene Gulf of Mexico. *Geology*, *40*, 1119–1122.

Kirk, H. J. C. (1957). The geology and mineral resources of the Upper and adjacent areas. Geological Survey department British territories in Borneo, Memoir 8.

Kneller, B. C., & Buckee, C. (2000). The structure and fluid mechanics of turbidity currents: A review of some recent studies and their geological implications. *Sedimentology*, *47*, 62–94.

Kuenen, P. H. H. (1966). Matrix of turbidites: Experimental Approach. *Sedirnentology*, *7*, 261–291.

Liechti, P., Roe, F. W., & Haile, N. S. (1960). The geology of Sarawak, Brunei and the western part of North Borneo. Geological Survey department British territories in Borneo, Bulletin, 3, Kuching.

Lowe, D. R. (1982). Sediment gravity flows: II. Depositional models with special reference to the deposits of high-density turbidity currents. *Journal of Sedimentology Petrology*, *52*, 279–297.

Lowe, D. R., & Guy, M. (2000). Slurry-flow deposits in the Britannia Formation (Lower Cretaceous), North Sea: A new perspective on the turbidity current and debris flow problem. *Sedimentology*, *47*, 31–70.

MacEachern, J. A., Bann, K. L., Pemberton, S. G., & Gingras, M. K. (2007). The Ichnofacies paradigm: High-resolution paleoenvironmental interpretation of the rock record, p. 49–85. In J. A. MacEachern, K. L. Bann, M. K. Gingras, & S. G. Pemberton (Eds.), *Applied ichnology*, Society for Sedimentary Geology Special Publication (Vol. 83) (pp. 27–64).

Madon, M. (1999). Basin types, tectono-stratiraphic provinces, structural styles. In: The Petroleum Geology of Resources of Malaysia, PETRONAS, Kuala Lumpur, (p. 90–94).

Magalhaes, P., & Tinterri, R. (2010). Stratigraphy and depositional setting of slurry and contained (reflected) beds in the Marnoso-arenacea Formation (Langhian-Serravallian) Northern Apenninnes, Italy. *Sedimentology*, *57*, 1685–1720.

Marini, M., Milli, S., & Moscatelli, M. (2011). Facies and architecture of 711 the Lower Messinian turbidite complexes from the Laga Basin (central Apennines, Italy). *Journal of Mediterranean Earth Science*, *3*, 45–72.

Masson, D. G., Van Niel, B., & Waever, P. P. E. (1997). Flow processes and sediment deformation in the Canary Debris Flow on the NW African Continental Rise. *Sedimentary Geology*, *110*, 163–179.

Middleton, G. V., & Hampton, M. A. (1973). Sediment gravity flows: Mechanics of flow and deposition, in turbidites and deep-water sedimentation: Society of Economic Paleontologists Mineralogists, Pacific Section Short Course Lecture Notes, (p. 1–38).

Migeon, S., Savoye, B., Zanella, E., Mulder, T., Faugeres, J.-C., & Weber, O. (2001). Detailed seismic and sedimentary study of turbidite sediment waves on the Var Sedimentary Ridge (SE France): Significance for sediment transport and for the mechanism of sediment wave construction. *Marine and Petroleum Geology*, *18*, 179–208.

Moss, S. J. (1998). Embaluh group turbidites in Kalimantan evolution of a remnant oceanic basin in Borneo during the late Cretataceous to Paleogene. *Journal of the Geological Society, London*, *155*, 509–524.

Mueller, P., Patacci, M., & Giulio, A. D. (2017). Hybrid event beds in the proximal to distal extensive lobe domain of the coarse-grained and sand-rich Bordighera turbidite system (NW Italy). *Marine and Petroleum Geology*, *86*, 908–931.

Mulder, T., & Alexander, J. (2001). The physical character of subaqueous sedimentary density flows and their deposits. *Sedimentology*, *48*(2), 269–299.

Mulder, T., Zaragosi, S., Razin, P., Grelaud, C., Lanfumy, V., & Bavoil, F. (2009). A new conceptual model for the deposition process of homogenite: Application to a Cretaceous megaturbidite of the western Pyrenees (Basque region, SW France). *Sedimentary Geology*, *222*, 263–273.

Mutti, E. (1974). Examples of ancient deep-sea fan deposits from circum Mediterranean geosynclines in modern and ancient geosynclinal sedimentation. In R. H. Dott, Jr., & R. H. Shaver (Eds.), *Modern and ancient geosynclinals sedimentation*. *Society of Economic Paleontologists and Mineralogists*, Special Publications, (Vol. **19**). (pp. 92–105).

Mutti, E. (1992). *Turbidite sandstones*. *San Donato Milanese, Agip, Istituto di Geologia*. (p. 275). Parma: Universita di Parma.

Mutti, E., Ricci Lucchi, F., & Roveri, M. (2002). Revisiting turbidites of the Marnoso-arenacea Formation and their basin-margin equivalents: Problems with classic models. Excursion Guidebook, Workshop organized by Dipartimento di Scienze della Terra (Universita` di Parma) and Eni- Divisione Agip, 64th EAGE Conference and Exhibition, (p. 120). 27–30 May, Florence, Italy, p.120.

Nelson, C. H., Twichell, D. C., Schwab, W. C., Lee, H. J., & Kenyon, N. H. (1992). Upper Pleistocene turbidite sand beds and chaotic silt beds in the channelized, distal, outer-fan lobes of the Mississippi fan: Geology, (Vol. 20) (p. 693–696).

Patacci, M., Haughton, P. D. W., & McCaffrey, W. D. (2014). Rheological complexity in sediment gravity flows forced to decelerate against a confining slope, Braux, E France. *Journal of Sedimentary Reasearch*, *84*(4), 270–277.

Pickering, K. T. (1981). Two types of outer fan lobe sequence, from the late Precambrian Kongsford Formation submarine fan, Finnmark, north Norway. *Journal of Sedimentary Petrology*, *51*, 1277–1286.

Pierce, C. S., Haughton, P. D. W., Shannon, P. M., Pulham, A. J., Barker, S. P., & Martinsen, O. J. (2017). Variable character and diverse origin of hybrid event beds (HEBs) in a sandy submarine fan system, Pennsylvanian Ross Sandstone Formation, western Ireland. *Sedimentology*, *65*(3), 952–992.

Piper, D. J. W. (1978). Turbidite muds and silts on deep sea fans and abyssal plains. In D. J. Stanley, & G. Kelling (Eds.), *Sedimentation in submarine canyons, fans and trenches* (pp. 163–176). Pennsylvania: Dowden, Hutchinson and Ross, Stroudsburg.

Pirmez, C., Beauboeul, R. T., Friedmann, S. J., & Mohrig, D. C. (2000). Equilibrium profile and base level in submarine channels: Examples from Late Pleistocene systems and implications for the architecture of deep-water reservoirs. In P. Weimer, R. M. Slatt, A. H. Bouma, & D. T. Lawrence (Eds.), *Gulf Coast Section, SEPM, 20th Annual research Conference: Deep-water reservoirs of the world* (pp. 782–805).

Prélat, A., Covault, J. A., Hodgson, D. M., Fildani, A., & Flint, S. S. (2010). Intrinsic controls on the range of volumes, morphologies, and dimensions of submarine lobes. *Sedimentary Geology*, *232*, 658–674.

Prélat, A., & Hodgson, D. M. (2013). The full range of turbidite bed thickness patterns in submarine lobes: Controls and implications. *Journal of the Geological Society*, *170*(1), 209–214.

Prélat, A., Hodgson, D. M., & Flint, S. S. (2009). Evolution, architecture and hierarchy of distributary deep-water deposits: A high-resolution outcrop investigation from the Permian Karoo Basin, South Africa. *Sedimentology*, *56*, 2132–2154.

Rangin, C., Bellon, H., Benard, F., Letouzey, J., Muller, C., & Sanudin, T. (1990). Neogene arc-continent collision is Sabah, N. Borneo (Malaysia). *Tectonophysics*, *183*, 305–319.

Ricci-Lucchi, F. (1975). Depositional cycles in two turbidite formations of northern Apennines (Italy). *Journal of Sedimentary Petrology*, *45*, 3–43.

Shanmugam, G. (2013). Modern internal waves and internal tides along oceanic pycnoclines: Challenges and implications for ancient deep-marine baroclinic sands. *American Association of Petroleum Geologists Bulletin*, *97*, 767–811.

Shipp, R. C., Weimer, P., & Posamentier, H. (2011). Mass transport deposits in deepwater setting. *SEPM Special Publication*, *96*, 161.

Southern, S. J., Kane, I. A., Warchoł, M. J., Porten, K. W., & McCaffrey, W. D. (2017). Hybrid event beds dominated by transitional-flow facies: Character, distribution and significance in the Maastrichtian Springar Formation, north-west Vøring Basin, Norwegian Sea. *Sedimentology*, *64*(3), 747–776.

Spychala, Y. T., Hodgson, D. M., & Lee, D. R. (2017). Autogenic controls on hybrid bed distribution in submarine lobe complexes. *Marine and Petroleum Geology*, *88*, 1078–1093.

Spychala, Y. T., Hodgson, D. M., Prelat, A., Kane, I. A., Flint, S. S., & Mountney, N. P. (2017). Frontal and lateral submarine lobe fringes: Comparing sedimentary facies, architecture and flow processes. *Journal of Sedimentary Research*, *87*(1), 75–96.

Stacey, M. W., & Bowen, A. J. (1988). The vertical structure of density and turbidity currents: Theory and observations. *Journal of Geophysical Research*, *93*(C4), 3528–3542.

Stow, D. A. V., & Bowen, A. J. (1978). Origin of lamination in deep sea, fine-grained sediments. *Nature*, *274*, 324–328.

Stow, D. A. V., & Bowen, A. J. (1980). A physical model for the transport and sorting of fine-grained sediment by turbidity currents. *Sedimentology*, *27*, 31–46.

Sumner, E. J., Amy, L., & Talling, P. J. (2008). Deposit structure and processes of sand deposition from a decelerating sediment suspension. *Journal of Sedimentary Research*, *78*, 529–547.

Sumner, E. J., Talling, P. J., & Amy, L. A. (2009). Deposits of flows transitional between turbidity current and debris flow. *Geology*, *37*, 991–994.

Sylvester, Z., & Lowe, D. R. (2004). Textural trends in turbidites and slurry beds from the Oligocene flysch of the Carpathians, Romania. *Sedimentology*, *51*, 945–972.

Talling, P. J. (2013). Hybrid submarine flows comprising turbidity current and cohesive debris flow: Deposits, theoretical and experimental analyses, and generalized models. *Geosphere*, *9*, 460–488.

Talling, P. J., Amy, L. A., & Wynn, R. B. (2007). New insights into the evolution of large volume turbidity currents: Comparison of turbidite shape and previous modelling results. *Sedimentology*, *54*, 737–769.

Talling, P. J., Amy, L. A., Wynn, R. B., Blackbourn, G., & Gibson, O. (2007). Turbidity current evolution deduced from extensive thin turbidites: Marnoso-arenacea Formation (Miocene), Italian Apennines. *Journal of Sedimentary Research*, *77*, 172–196.

Talling, P. J., Amy, L. A., Wynn, R. B., Peakall, J., & Robinson, M. (2004). Beds comprising debrite sandwiched within co-genetic turbidite: Origin and widespread occurrence in distal depositional environments. *Sedimentology*, *51*, 163–194.

Talling, P. J., Masson, D. G., Sumner, E. J., & Malgesini, G. (2012). Subaqueous sediment density flows: Depositional processes and deposits types. *Sedimentology*, *59*, 1937–2003.

Talling, P. J., Wynn, R. B., Masson, D. G., Frenz, M., Cronin, B. T., Schiebel, R., … Amy, L. A. (2007). Debris flow deposition from giant submarine flow begins far away from original landslide. *Nature*, *450*, 541–544.

Tan, D. N. K. (1979). Lupar Valley, West Sarawak Malaysia. Geological survey of Malaysia report, 13.

Tan, D. N. K. (1982). The Lubok Antu Melange, Lupar Valley, West Sarawak: A lower tertiary subduction complex. *Geological Society of Malaysia Bulletin*, *15*, 31–46.

Tate, R. B. (2001). Geological map of Borneo Island, CD-Rom published by the Geological Society of Malaysia, Kuala Lumpur.

Taylor, A. M., & Goldring, R. (1993). Description and analysis of bioturbation and ichnofabric. *Journal of the Geological Society, London*, *150*, 141–148.

Terlaky, V., Rocheleau, J., & Arnott, W. C. (2016). Stratal composition and stratigraphic organization of stratal elements in an ancient deep-marine basin-floor succession, Neoproterozoic Windermere Supergroup, British Columbia, Canada. *Sedimentology*, *63*, 136–175.

Tinterri, R., Muzzi Magalhaes, P. M., Tagliaferri, A., & Cunha, R. S. (2016). Convolute laminations and load structures in turbidites as indicators of flow reflections and decelerations against bounding slopes. Examples from the Marnoso-arenacea Formation (northern Italy) and Annot Sandstones (south eastern France). *Sedimentary Geology*, *344*, 382–407.

Tongkul, F. (1997). Sedimentation and tectonics of Paleogene sediments in central Sarawak. *Geology Society of Malaysia Bulletin*, *40*, 135–155.

Vinnels, J. S., Butler, R. W., McCaffrey, W. D., & Lickorish, W. H. (2010). Sediment distribution and architecture around a bathymetrically complex basin: An example from the eastern Champsaur Basin, SE France. *Journal Sedimentary Research*, *80*, 216–235.

Wolfenden, E. B. (1960). The geology and mineral resources of the Lower Rajang valley and adjoining areas, Sarawak. Geological Survey department British territories in Borneo. *Memoir*, *11*.

Wood, A., & Smith, A. J. (1958). The sedimentation and sedimentary history of the Aberystwyth grits (upper Llandoverian). *Geological Society of London, Quarterly Journal*, *114*, 163–195.

Zainol, A. A. B., Madon, M., & Abdul Jalil, M. (2007). Deep-marine sedimentary facies in the Belaga Formation (Cretaceous-Eocene), Sarawak: Observations from new outcrops in the Sibu and Tatau areas. *Geological Society of Malaysia, Bulletin*, *53*, 35–45.

Zhang, J. J., Wu, S. H., Fan, T. E., Fan, H. J., Jiang, L., Chen, C., … Lin, P. (2016). Research on the architecture of the submarine-fan lobes in the Niger Delta Basin, Offshore West Africa. *Journal of Palaeogeography*, *5*(3), 185–204.

How to cite this article: Kuswandaru GY, Amir Hassan MH, Matenco LC, Taib NI, Mustapha KA. Turbidite, debrite, and hybrid event beds in submarine lobe deposits of the Palaeocene to middle Eocene Kapit and Pelagus members, Belaga Formation, Sarawak, Malaysia. *Geological Journal*. 2019;54:3421–3437. https://doi.org/10.1002/gj.3347